Journal Pre-proof

An asymptotically compatible probabilistic collocation method for randomly heterogeneous nonlocal problems

Yiming Fan, Xiaochuan Tian, Xiu Yang, Xingjie Li, Clayton Webster et al.

Please cite this article as: Y. Fan, X. Tian, X. Yang et al., An asymptotically compatible probabilistic collocation method for randomly heterogeneous nonlocal problems, *Journal of Computational Physics*, 111376, doi: https://doi.org/10.1016/j.jcp.2022.111376.

An asymptotically compatible probabilistic collocation method for randomly heterogeneous nonlocal problems

Yiming Fan[a], Xiaochuan Tian[b], Xiu Yang[c], Xingjie Li[d], Clayton Webster[e], Yue Yu[a]

[a]*Department of Mathematics, Lehigh University, Bethlehem, PA, 18015*
[b]*Department of Mathematics, University of California, San Diego, CA, 92093*
[c]*Department of Industrial and Systems Engineering, Lehigh University, Bethlehem, PA, 18015*
[d]*Department of Mathematics and Statistics, University of North Carolina at Charlotte, Charlotte, NC, 28223*
[e]*Department of Mathematics, University of Texas at Austin, Austin, TX, 78712*

Abstract

In this paper we present an asymptotically compatible meshfree method for solving nonlocal equations with random coefficients, describing diffusion in heterogeneous media. In particular, the random diffusivity coefficient is described by a finite-dimensional random variable or a truncated combination of random variables with the Karhunen-Loève decomposition, then a probabilistic collocation method (PCM) with sparse grids is employed to sample the stochastic process. On each sample, the deterministic nonlocal diffusion problem is discretized with an optimization-based meshfree quadrature rule. In terms of analysis, we first show the analytic regularity of solutions with respect to parameters in the diffusion coefficients and then present the rigorous convergence analysis for the proposed numerical scheme, i.e., the scheme is asymptotic compatible spatially and achieves an algebraic or sub-exponential convergence rate in the random coefficients space as the number of collocation points grows. These results are further confirmed by a number of benchmark problems. Finally, to validate the applicability of this approach we consider a randomly heterogeneous nonlocal problem with a given spatial convention structure, demonstrating that the proposed PCM approach achieves substantial speed-up compared to conventional Monte Carlo simulations.

Keywords: Uncertainty Quantification, Analytic Regularity, Asymptotic Compatibility, Meshfree Method, Nonlocal Diffusion Problem, Probabilistic Collocation, Stochastic Method

Contents

1. Introduction

Since the last decade, there has been a great interest in using nonlocal integro-differential equations to describe physical systems, due to their natural ability to describe physical phenomena at small scales and their reduced regularity requirements which lead to greater flexibility [1–23]. These nonlocal models are defined in terms of a lengthscale δ, referred to as a horizon, which denotes the extent of nonlocal interaction. The nonlocal viewpoint allows a natural description of processes requiring reduced regularity in the relevant solution, such as the peridynamics model for fracture mechanics [2, 24, 25]. An important feature of such models is that they revert back to corresponding classical partial differential equation (PDE) models as the horizon $\delta \to 0$. When refining the spatial discretization characterized by grid size h such that $h \to 0$, discretization methods which preserve correct local limits are termed asymptotically compatible (AC) schemes [26], and there has been significant work in recent years toward establishing such discretizations, see, e.g., [26–36]. Broadly, strategies either involve adopting traditional weak form via finite element shape functions and carefully performing geometric calculations to integrate over relevant horizon/element subdomains, or adopting a strong form meshfree discretization where particles are associated with abstract measure [37]. The former is more amenable to mathematical analysis due to a better variational setting, while the latter is simple to implement and generally with smaller computational cost [38, 39]. In this work we pursue the asymptotically compatible meshfree approach.

One of the limitations of the current state-of-the-art works is that most of them consider a homogenized nonlocal model, which may not work well when the material is heterogeneous and its microsctructure plays a critical role. In a recent study [40], Zhao et al. found that a fully homogenized peridynamic model fails

to capture certain correct fracture modes/patterns in reinforced concrete. Therefore, they have proposed a stochastic bond-based peridynamic model where the material property is described as random fields. The type of each bond connecting material points $\boldsymbol{x}$ and $\boldsymbol{y}$ was modeled by a random variable, and the discrete probability distribution of this random variable depends on the volume fraction of aggregate and cement on $\boldsymbol{x}$ and $\boldsymbol{y}$. With this model, fracture patterns and the order in which various cracks develop match experimental observations. Their findings indicate the importance of considering the spatial variability of material properties in nonlocal models, especially when the physical parameters describing spatially varying properties of heterogeneous materials cannot be accurately characterized in all details.

In the present paper, we consider a stochastic nonlocal diffusion equation, where the heterogeneous material property is modeled by a random field. The solution of this stochastic equation describes the probability density function (PDF) of the state variable, e.g., the concentration. Differing from [40] which studied the solution pattern on each individual realization rather than the solution statistics, we focus on the numerical estimates of the first two statistical moments, i.e., the mean and covariance. The mean provides an unbiased estimate of the variables and the variance quantifies the uncertainty associated with this estimate. The Monte Carlo (MC) method and its variations [41–45] are usually used to solve stochastic moment equations and often considered a reliable numerical tool [46]. In the MC method, a large number (denoted by K) of random realizations (samples) are generated for the prescribed random inputs and repetitive deterministic solvers are employed for each sample. The results are then statistically analyzed based on all K samples to calculate leading moments of variables of interest. However, its slow $O(K^{-1/2})$ convergence rate hinders the application of MC method on relatively large scale problems, since one has to solve the differential equation for every sample. Moreover, comparing with local (classical) PDE models, numerically solving nonlocal equations is often more expensive due to its relative lack of sparsity. Therefore, the need for efficient and accurate stochastic numerical methods is even more pressing in the nonlocal setting.

To achieve a faster convergence rate, several stochastic numerical methods were developed for stochastic local (classical) PDE models including probabilistic Galerkin methods (PGMs) [47–53], probablistic colloca-tion methods (PCMs) [54–58], reduced basis methods [59–64], etc. Among these methods, the probabilistic collocation method with sparse grids inherits the ease of implementation in the MC methods since only solutions at sample points are needed. At the same time, it also reduces the required number of sample points to achieve a given numerical accuracy, especially on problems with small random dimensions and suf-ficient solution smoothness in the parameter space. Therefore, in this work we will employ the probabilistic collocation methods with sparse grids. Comparing with the attentions received by stochastic PDE problems, numerical studies of nonlocal problems in the uncertainty quantification setting remain limited. In [64], reduced-basis methods are developed for constructing surrogates of the solution of a parameterized nonlocal diffusion problem with random input data in a finite element method framework. However, to the authors' best knowledge, there exists no work on studying the solution smoothness and the theoretical limiting be-havior of stochastic nonlocal problems when $\delta \to 0$, while these studies are crucial to the design of accurate

3

and asymptotically compatible stochastic numerical schemes. Moreover, the application and rigorous error estimates of meshfree discretization method also remain limited for stochastic nonlocal problems.

The major contribution of the present work is to propose a complete workflow of asymptotically compatible stochastic numerical methods and rigorous mathematical analysis for randomly heterogeneous nonlocal diffusion problems. In particular, we propose to employ a meshfree method with optimization-based quadrature rule [33, 37] for the discretization in the physical space, and a PCM with sparse grids for the discretization in the parameter space. By proving that the solution of the nonlocal equation with diffusivity coefficient described as a finite-dimensional random field is analytic in the input random variables, we show that the sparse grid PCM achieves at least algebraic convergence with the increase of sample points. Moreover, given sufficiently large level of sparse grid formulation, the sparse grid PCM converges sub-exponentially. To characterize the convergence in physical space and the asymptotic compatibility, we for the first time provide analysis for the stochastic nonlocal diffusion problem with random coefficients, showing that its solution converges to the local solution when $\delta \to 0$. Based on these mathematical analysis, we provide error estimates for the optimization-based quadrature rule with both fixed horizon δ and also δ going to an asymptotic limit. In particular, we show that as far as the corresponding local solution has C^4 regularity spatially, the nonlocal numerical solution converges to the analytical local solution with an $O(\delta^2)$ convergence rate as $\delta \to 0$. When the nonlocal solution has C^1 regularity spatially and consider a fixed δ, the nonlocal numerical solution converges to the analytical nonlocal solution with an $O(h)$ convergence rate as the grid size $h \to 0$. Lastly, we develop a complete workflow to solve for randomly heterogeneous nonlocal problems, by representing the heterogeneous material coefficient as a random field with given spatial correlation structure and approximating the coefficient by a truncated combination of random variables using the Karhunen-Loève expansion. This work provides a road map to add uncertainty quantification functionality onto pre-existing asymptotically compatible code for deterministic nonlocal problems in a non-intrusive manner, which achieves algebraic or sub-exponential convergence in the solution mean and variance while sustaining the spatial asymptotic compatibility to the correct local limit. Furthermore, we notice that the regularity requirements for the nonlocal and local solutions in our error estimates are not guaranteed in some real-world applications. Therefore, we also investigate the numerical convergence when these requirements are not satisfied and provide empirical convergence rates.

We remark that the paper is organized to establish the rigorous mathematical underpinnings of the approach in the first half, while the second half focuses on a numerical verification and more engineering-oriented exploration of its application, especially on the cases that are not covered by the theoretical error estimates. The paper is organized as follows, with all major notations listed in Table 1. We recall first the relevant results in nonlocal calculus and provide mathematical analysis for the deterministic and stochastic nonlocal diffusion problems in Section 2. After establishing the continuous limits of the stochastic nonlocal problem, we next pursue a consistent discretization. In Section 3, we propose our numerical approach for stochastic nonlocal problems by employing the sparse grid PCM and an optimization-based meshfree

4

quadrature rule in the physical space and establish rigorous error estimates. In particular, we show that the proposed approach achieves algebraic or sub-exponential convergence in the parametric space, and address the convergence rates to the nonlocal and local limits respectively. The theoretical error estimates are verified on a number of one-dimensional and two-dimensional problems with analytic solutions for the local and nonlocal limits in Section 4. In Section 5, we further extend the proposed formulation to handle a more engineering-oriented problem, where the random diffusivity coefficient is modeled by a random field with a given spatial correlation structure. Section 6 summarizes our findings and discusses future research.

2. The Deterministic and Parametric Nonlocal Diffusion Problem

In this section we introduce the major notations and definitions will be used throughout this paper. We begin with Table 1 and in Section 2.1 we introduce the deterministic nonlocal diffusion problem while Section 2.2 is dedicated to the stochastic nonlocal diffusion problem. Moreover, we provide novel theoretical analysis for the stochastic nonlocal diffusion problem, namely, its compatibility with the classical companion and analytic regularity.

2.1. Nonlocal Calculus and Deterministic Nonlocal Diffusion Problem

In this section, we review the the governing equations of deterministic nonlocal diffusion models which provide the foundation for the stochastic nonlocal problems of interest. Given that $\Omega \subset \mathbb{R}^d$, $d \in \mathbb{Z}^+$, is a bounded Lipschitz domain, we consider the nonlocal elliptic equation in Ω. To do so, we first introduce the relevant nonlocal calculus. Let $\boldsymbol{\alpha}(\boldsymbol{x}, \boldsymbol{y}) : \mathbb{R}^d \times \mathbb{R}^d \to \mathbb{R}^d$ be an antisymmetric function, for a vector function $\boldsymbol{v}(\boldsymbol{x}, \boldsymbol{y}) : \mathbb{R}^d \times \mathbb{R}^d \to \mathbb{R}^d$, we define the nonlocal divergence $\mathcal{D}[\boldsymbol{v}] : \mathbb{R}^d \to \mathbb{R}$:

$$\mathcal{D}[\boldsymbol{v}](\boldsymbol{x}) := \int_{\mathbb{R}^d} (\boldsymbol{v}(\boldsymbol{x}, \boldsymbol{y}) + \boldsymbol{v}(\boldsymbol{y}, \boldsymbol{x})) \cdot \boldsymbol{\alpha}(\boldsymbol{x}, \boldsymbol{y}) d\boldsymbol{y}, \quad \boldsymbol{x} \in \mathbb{R}^d,$$

and for a scalar function $u(\boldsymbol{x}) : \mathbb{R}^d \to \mathbb{R}$ we define the nonlocal gradient $\mathcal{G}[u] : \mathbb{R}^d \times \mathbb{R}^d \to \mathbb{R}^d$:

$$\mathcal{G}[u](\boldsymbol{x}, \boldsymbol{y}) := (u(\boldsymbol{y}) - u(\boldsymbol{x})) \boldsymbol{\alpha}(\boldsymbol{x}, \boldsymbol{y}), \quad \boldsymbol{x}, \boldsymbol{y} \in \mathbb{R}^d.$$

As shown in [21], the adjoint operator of $\mathcal{D}$ with respect to the L^2 inner product is $\mathcal{D}^* = -\mathcal{G}$. We then consider a nonlocal diffusion problem where every point $\boldsymbol{x} \in \Omega$ is interacting with a neighborhood of points, and their interaction is described by a symmetric kernel function $\gamma(\boldsymbol{x}, \boldsymbol{y}) := \boldsymbol{\alpha}(\boldsymbol{x}, \boldsymbol{y}) \cdot \boldsymbol{\alpha}(\boldsymbol{x}, \boldsymbol{y})$ and a two-point scalar function $A(\boldsymbol{x}, \boldsymbol{y})$ representing the nonlocal diffusion strength. Without loss of generality, we assume in this paper that A is symmetric in its two arguments, i.e., $A(\boldsymbol{x}, \boldsymbol{y}) = A(\boldsymbol{y}, \boldsymbol{x})$. A nonlocal diffusion operator on a scalar function $u : \mathbb{R}^d \to \mathbb{R}$ is then given by

$$\mathcal{L}[u](\boldsymbol{x}) := \mathcal{D}[A(\boldsymbol{x}, \boldsymbol{y})\mathcal{G}[u]](\boldsymbol{x}) = 2 \int_{\mathbb{R}^d} A(\boldsymbol{x}, \boldsymbol{y})\gamma(\boldsymbol{x}, \boldsymbol{y})(u(\boldsymbol{y}) - u(\boldsymbol{x})) d\boldsymbol{y}, \quad \boldsymbol{x} \in \mathbb{R}^d.$$

5

Symbol	Description
Ω	Physical domain.
δ	Horizon size.
$B_\delta(\boldsymbol{x}) = \{\boldsymbol{y} : |\boldsymbol{y} - \boldsymbol{x}| \le \delta\}$	The physical interaction region surrounding $\boldsymbol{x}$.
Ω_δ	Nonlocal boundary which is a collar of thickness surrounding Ω.
$(\Omega_p, \mathcal{F}, \mathcal{P})$	Probability space.
Γ	Space of random variables.
d	Dimension of the physical space Ω.
N	Dimension of the random space, i.e., the number of random variables.
M	Total number of grid points for spatial discretization.
K	Total number of collocation points (samples) in PCM.
$\mathcal{D}$	Nonlocal divergence operator.
$\mathcal{G}$	Nonlocal gradient operator.
$\mathcal{L}^\delta$	Nonlocal diffusion operator.
$\mathcal{L}^0$	Local (classical) diffusion operator.
$\mathcal{L}_h^\delta$	Discretized nonlocal diffusion operator.
$v_{(i)}$	The i-th component of vector $\boldsymbol{v}$.
$M_{(i,j)}$	The i-th row j-th column element of matrix $\boldsymbol{M}$.
$u^D : \Omega_\delta \to \mathbb{R}$	Dirichlet type boundary condition.
$\gamma(\boldsymbol{x}, \boldsymbol{y}) = \gamma_\delta(|\boldsymbol{y} - \boldsymbol{x}|)$	Symmetric kernel function.
s	Order of singularity in kernel γ.
$A : (\Omega \cup \Omega_\delta) \times (\Omega \cup \Omega_\delta) \times \Gamma \to \mathbb{R}$	Nonlocal random diffusion strength function.
$a : \Omega \times \Gamma \to \mathbb{R}$	Local random diffusion strength function.
r and R	Lower and upper bounds of A and a.
$S_\delta(\Omega)$ and T_δ	Nonlocal energy space and the corresponding bilinear form.
$\rho : \Gamma \to \mathbb{R}^+$	Probability density of the random variable.
$\chi_h = \{\boldsymbol{x}_i\}$ and h	(Quasi-uniform) grid set and the grid size for spatial discretization.
$\boldsymbol{V}_{h,\boldsymbol{x}_i}$	Space of functions to be integrated exactly in the spatial discretization.
$\omega_{j,i}$	Quadrature weight for $\boldsymbol{x}_j$ to generate integral in $B_\delta(\boldsymbol{x}_i)$.
$\Theta_N = \{\boldsymbol{\xi}_k\}$	Prescribed nodes for the Lagrange interpolation in the random space Γ.
μ_k	Corresponding quadrature weight for $\boldsymbol{\xi}_k$ in the random space.
ζ	Sparseness parameter for the Smolyak sparse grid formulation.
$\eta = \zeta + N$	Level of the Smolyak sparse grid formulation.
ϕ^ϵ	Mollification function.
$u^\delta : (\Omega \cup \Omega_\delta) \times \Gamma \to \mathbb{R}$	Nonlocal solution of (2.12).
$u^0 : \Omega \times \Gamma \to \mathbb{R}$	Local solution of (2.15).
u_h^δ	Numerical solution for the deterministic nonlocal diffusion problem.
$u_{h,K}^\delta$	Numerical solution with spatial grid set χ_h and sparse grid level η in PCM.
$\Xi(\boldsymbol{x}, \boldsymbol{y})$	Covariance kernel for the variances between material points $\boldsymbol{x}$ and $\boldsymbol{y}$.

Table 1: Table of Notations.

In this paper we further assume that the interacting kernel function γ is radial and compactly supported on a Euclidean ball surrounding $\boldsymbol{x}$, i.e., $B_\delta(\boldsymbol{x}) := \{\boldsymbol{y} \in \mathbb{R}^d : |\boldsymbol{y} - \boldsymbol{x}| < \delta\}$:

$$\begin{cases} \gamma(\boldsymbol{x}, \boldsymbol{y}) = \gamma_\delta(|\boldsymbol{x} - \boldsymbol{y}|) = \frac{1}{\delta^{d+2}}\gamma_1\left(\frac{|\boldsymbol{x}-\boldsymbol{y}|}{\delta}\right) = \frac{D_0}{\delta^{d+2-s}|\boldsymbol{x}-\boldsymbol{y}|^s} \\ \text{where } \gamma_1 \text{ is a nonnegative and nonincreasing function with } s\text{-th order singularity, satisfying} \\ \text{supp}(\gamma_1) \subset B_1(\boldsymbol{0}) \text{ and } \int_{B_1(\boldsymbol{0})} \gamma_1(|\boldsymbol{z}|)|\boldsymbol{z}|^2 d\boldsymbol{z} = d. \end{cases} \quad (2.1)$$

Here, we also require that the kernel γ is integrable, i.e. $s \in [0, d)$. As will be seen in the mathematical analysis of Section 2 and Section 3, this requirement makes the proposed meshfree method well-defined and converging. The above kernel assumptions also have implications on the boundary conditions that are prescribed on a collar of thickness δ outside the domain Ω, that we denote as

$$\Omega_\delta := \left\{\boldsymbol{x} \in \mathbb{R}^d \backslash \Omega : \text{dist}(\boldsymbol{x}, \partial\Omega) < \delta\right\}$$

and refer to as nonlocal boundary.

Therefore, the static nonlocal diffusion problem in a deterministic parameters setting is given as:

$$\begin{cases} -\mathcal{L}^\delta[u](\boldsymbol{x}) = -\mathcal{D}[A(\boldsymbol{x}, \boldsymbol{y})\mathcal{G}[u]](\boldsymbol{x}) = f(\boldsymbol{x}), & \text{for } \boldsymbol{x} \in \Omega \\ u(\boldsymbol{x}) = u^D(\boldsymbol{x}), & \text{for } \boldsymbol{x} \in \Omega_\delta, \end{cases} \quad (2.2)$$

where u^D is the given Dirichlet-type boundary datum in the nonlocal trace space [65]. Without loss of generality, for the analysis, we consider homogeneous Dirichlet boundary conditions $u^D(\boldsymbol{x}) = 0$, and the proposed method is applied to inhomogeneous Dirichlet-type problems in numerical tests of Section 4. Note that although the proposed model can be applied to other boundary conditions, e.g., the Neumann-type boundary conditions in [34, 35], here we focus on the Dirichlet-type nonlocal constraint problem for simplicity.

To make the nonlocal diffusion problem (2.2) uniformly elliptic, we make the uniform boundedness assumption on the diffusion coefficient $A(\boldsymbol{x}, \boldsymbol{y})$:

$$A \in L^\infty((\Omega \cup \Omega_\delta)^2), \text{ and } 0 < r \leq A(\boldsymbol{x}, \boldsymbol{y}) \leq R < \infty, \text{ for } \boldsymbol{x}, \boldsymbol{y} \in \Omega \cup \Omega_\delta, \quad (2.3)$$

where r and R are two positive constants. (2.2) is then associated with the nonlocal energy semi-norm

$$|u|^2_{S_\delta(\Omega)} = \int_{\Omega \cup \Omega_\delta} \int_{\Omega \cup \Omega_\delta} \gamma_\delta(|\boldsymbol{y} - \boldsymbol{x}|)(u(\boldsymbol{y}) - u(\boldsymbol{x}))^2 d\boldsymbol{y}d\boldsymbol{x}$$

where the nonlocal energy space is defined as

$$S_\delta(\Omega) = \left\{u \in L^2(\Omega \cup \Omega_\delta) : \int_{\Omega \cup \Omega_\delta} \int_{\Omega \cup \Omega_\delta} \gamma_\delta(|\boldsymbol{y} - \boldsymbol{x}|)(u(\boldsymbol{y}) - u(\boldsymbol{x}))^2 d\boldsymbol{y}d\boldsymbol{x} < \infty, \; u|_{\Omega_\delta} = 0\right\}.$$

Moreover, we define the bilinear form $T_\delta : S_\delta \times S_\delta \to \mathbb{R}$ as

$$T_\delta[v,w] = \int_{\Omega \cup \Omega_\delta} \int_{\Omega \cup \Omega_\delta} A(\boldsymbol{x}, \boldsymbol{y})\gamma_\delta(|\boldsymbol{x} - \boldsymbol{y}|)(v(\boldsymbol{y}) - v(\boldsymbol{x}))(w(\boldsymbol{y}) - w(\boldsymbol{x}))d\boldsymbol{y}d\boldsymbol{x}.$$

With the boundedness assumption proposed in (2.3) we have $0 < r|v|^2_{S_\delta(\Omega)} \le T_\delta[v,v] \le R|v|^2_{S_\delta(\Omega)}$. Notice that to solve for the weak solution of (2.2), we find $u(\boldsymbol{x}) \in S_\delta(\Omega)$ such that

$$T_\delta[u,v] = (f,v)_{L^2(\Omega)}, \quad \forall v \in S_\delta(\Omega). \tag{2.4}$$

As proved in [66], the bilinear form T_δ holds uniform ellipticity as well as the nonlocal Poincaré inequality, and therefore the weak formulation for the deterministic nonlocal equation (2.4) is well-posed. Here we summarize the relevant results in the following lemma:

Lemma 2.1. *[66, Proposition 5.3] Assume that $\gamma(\boldsymbol{x}, \boldsymbol{y})$ satisfies the conditions in (2.1), then there exist generic constants C and $\delta_0 > 0$ such that for all $0 < \delta < \delta_0$, the nonlocal energy semi-norm $|\cdot|_{S_\delta(\Omega)}$ satisfies the nonlocal Poincaré inequality*

$$||v||^2_{L^2(\Omega)} \le C|v|^2_{S_\delta(\Omega)}, \quad \forall v \in S_\delta(\Omega). \tag{2.5}$$

As a result of the Poincaré inequality, the semi-norm $|\cdot|_{S_\delta(\Omega)}$ defined is also a norm on $S_\delta(\Omega)$. For the rest of the paper, we will use $\|\cdot\|_{S_\delta(\Omega)} := |\cdot|_{S_\delta(\Omega)}$ to denote the norm on $S_\delta(\Omega)$. Combining Lemma 2.1 with the properties of A in (2.3), we can see that the bilinear form T_δ is bounded and coercive:

$$T_\delta[v,w] \le C||v||_{S_\delta(\Omega)}||w||_{S_\delta(\Omega)}, \quad \forall v,w \in S_\delta(\Omega), \tag{2.6}$$

$$T_\delta[v,v] \ge C||v||^2_{S_\delta(\Omega)}, \quad \forall v \in S_\delta(\Omega). \tag{2.7}$$

Therefore, by the Lax-Milgram theorem, there exists a unique solution $u^\delta \in S_\delta(\Omega)$ for the deterministic nonlocal diffusion problem (2.2) for each $f \in (S_\delta(\Omega))^*$, where $(S_\delta(\Omega))^*$ is the dual space of $S_\delta(\Omega)$ equipped with the induced norm $\|f\|_{(S_\delta(\Omega))^*} := \sup_{v \in S_\delta(\Omega), v \neq 0} \frac{\langle f,v \rangle}{\|v\|_{S_\delta(\Omega)}}$. $\langle \cdot, \cdot \rangle$ denotes the duality pairing between $(S_\delta(\Omega))^*$ and $S_\delta(\Omega)$, and $\langle f,v \rangle = (f,v)_{L^2(\Omega)}$ when $f \in L^2(\Omega) \subset (S_\delta(\Omega))^*$.

Next, we consider the compatibility of the nonlocal diffusion and the classical companion. To properly define the local limit of (2.2) as $\delta \to 0$, we need to make the following continuity assumption on the diffusion coefficient $A(\boldsymbol{x}, \boldsymbol{y})$:

$$A(\boldsymbol{x}, \boldsymbol{y}) \in C(\overline{(\Omega \cup \Omega_\delta)^2}) \text{ and } a(\boldsymbol{x}) := A(\boldsymbol{x}, \boldsymbol{x}). \tag{2.8}$$

Therefore, the nonlocal diffusion operator $\mathcal{L}^\delta[u]$ has a companion of the classical diffusion operator $-\nabla \cdot (a(\boldsymbol{x})\nabla(u(\boldsymbol{x})))$, and (2.2) can be seen as a nonlocal analogue to the local diffusion equation with Dirichlet-

type boundary condition:

$$
\begin{cases}
\mathcal{L}^0[u](\boldsymbol{x}) := -\nabla \cdot (a(\boldsymbol{x})\nabla(u(\boldsymbol{x}))) = f(\boldsymbol{x}), & \text{for } \boldsymbol{x} \in \Omega \\
u(\boldsymbol{x}) = u^D(\boldsymbol{x}), & \text{for } \boldsymbol{x} \in \partial\Omega,
\end{cases}
\tag{2.9}
$$

From (2.3), we have $0 < r \leq a(\boldsymbol{x}) \leq R$ for any $\boldsymbol{x} \in \Omega$, so (2.9) has a unique and bounded solution in $H^1(\Omega) := \{u \in L^2(\Omega) \big| \int_\Omega |\nabla u(\boldsymbol{x})|^2 d\boldsymbol{x} < \infty\}$ with corresponding boundary condition $u|_{\partial\Omega}(\boldsymbol{x}) = u^D(x)$. When we consider $u^D = 0$, the solution space is denoted by $H^1_0(\Omega) := \{u \in H^1(\Omega), u|_{\partial\Omega} = 0\}$.

Denoting the solution of local problem (2.9) as $u^0(\boldsymbol{x})$ and the solution of the nonlocal one (2.2) with a given horizon size δ as $u^\delta(\boldsymbol{x})$, we now show the convergence theorem.

Theorem 2.2. *Assume that $\gamma(\boldsymbol{x}, \boldsymbol{y})$ satisfies the conditions in (2.1), and $A(\boldsymbol{x}, \boldsymbol{y})$ satisfies the conditions in (2.3). Let $f \in (S_\delta(\Omega))^*$, the dual space of $S_\delta(\Omega)$, then we have*

$$
\|u^\delta\|_{S_\delta(\Omega)} \leq \frac{\|f\|_{(S_\delta(\Omega))^*}}{r}.
\tag{2.10}
$$

In addition, if $\|f\|_{(S_\delta(\Omega))^*}$ is uniformly bounded for all $\delta \in (0, \delta_0)$ and $A(\boldsymbol{x}, \boldsymbol{y})$ satisfies (2.8), then the nonlocal and local diffusion problems are compatitble as $\delta \to 0$:

$$
\lim_{\delta \to 0} \left\| u^\delta - u^0 \right\|_{L^2(\Omega)} = 0.
$$

Proof. We first show the proof of (2.10). Since u^δ is a solution to the nonlocal problem, we have

$$
T_\delta[u^\delta, v] = \langle f, v \rangle \leq \|f\|_{(S_\delta(\Omega))^*} \|v\|_{S_\delta(\Omega)}
$$

for any test function $v \in S_\delta(\Omega)$. Now let $v = u^\delta$, we get $r\|u^\delta\|^2_{S_\delta(\Omega)} \leq T_\delta[u^\delta, u^\delta] \leq \|f\|_{(S_\delta(\Omega))^*}\|u^\delta\|_{S_\delta(\Omega)}$. Therefore, we have (2.10).

The proof of the second part involves two steps. In the first step, we assume that $A(\boldsymbol{x}, \boldsymbol{y}) \in C^\infty((\Omega \cup \Omega_\delta)^2)$. Then it is easy to see by Taylor expansion that for any $v \in C_0^\infty(\Omega)$ (with zero extended values on Ω_δ), we have the pointwise convergence of $\mathcal{D}[A(\boldsymbol{x}, \boldsymbol{y})\mathcal{G}[u]](\boldsymbol{x})$ to $\nabla \cdot (a\nabla v(\boldsymbol{x}))$ as $\delta \to 0$. Indeed, by doing Taylor expansion of A and v around $\boldsymbol{x}$, we find that

$$
\mathcal{D}[A\mathcal{G}[v]](\boldsymbol{x}) = 2 \int A(\boldsymbol{x}, \boldsymbol{y})\gamma_\delta(|\boldsymbol{y} - \boldsymbol{x}|)(v(\boldsymbol{y}) - v(\boldsymbol{x}))d\boldsymbol{y}
$$

$$
= 2 \int \left(a(\boldsymbol{x}) + (\boldsymbol{y} - \boldsymbol{x}) \cdot \frac{\nabla a(\boldsymbol{x})}{2} \right) \gamma_\delta(|\boldsymbol{y} - \boldsymbol{x}|) \left((\boldsymbol{y} - \boldsymbol{x})^T \nabla v(\boldsymbol{x}) + \frac{1}{2}(\boldsymbol{y} - \boldsymbol{x})^T D^2 v(\boldsymbol{x})(\boldsymbol{y} - \boldsymbol{x}) \right) d\boldsymbol{y} + O(\delta^2)
$$

$$
= \nabla a(\boldsymbol{x}) \cdot \nabla v(\boldsymbol{x}) + a(\boldsymbol{x})\Delta v(\boldsymbol{x}) + O(\delta^2).
$$

Note that the above equalities are obtained since $\int_{B_\delta(\boldsymbol{x})} \gamma_\delta(|\boldsymbol{x} - \boldsymbol{y}|) \underset{i_1 + \cdots + i_d = 3}{\Pi} (\boldsymbol{y} - \boldsymbol{x})^{i_k}_{(k)} d\boldsymbol{y} = 0$ thanks to the symmetry of the kernel γ_δ, where $(\boldsymbol{y} - \boldsymbol{x})_{(k)}$ denotes the k-th component of $(\boldsymbol{y} - \boldsymbol{x})$ and $i_k \geq 0$ is

the power on that component. Then we argue that the convergence is also in $L^2(\Omega)$ since $|\mathcal{D}(A\mathcal{G}v)(\boldsymbol{x})|$ is uniformly bounded for $v \in C_0^\infty(\Omega)$ and $\delta \in (0, \delta_0)$. Notice that from the assumption on $\|f\|_{(S_\delta(\Omega))^*}$, we have $\|u^\delta\|_{S_\delta(\Omega)}$ being uniformly bounded for all $\delta \in (0, \delta_0)$. Then using similar arguments in [26], we can show $\|u^\delta - u^0\|_{L^2(\Omega)} \to 0$ as $\delta \to 0$.

For the general case that $A \in C(\overline{(\Omega \cup \Omega_\delta)^2})$, we will use the mollification technique. Take standard mollifiers $\phi^\epsilon \in C^\infty(\mathbb{R}^{2d})$, we define $A^\epsilon = \phi^\epsilon * A$. We denote the solution to (2.2) associated with coefficient A^ϵ to be $u^{\delta,\epsilon}$. Then we can use the first step to conclude that $\|u^{\delta,\epsilon} - u^{0,\epsilon}\|_{L^2(\Omega)} \xrightarrow{\delta \to 0} 0$, where $u^{0,\epsilon}$ is the solution to (2.9) associated with coefficient $a^\epsilon(\boldsymbol{x}) := A^\epsilon(\boldsymbol{x}, \boldsymbol{x})$. Now in order to show $\|u^\delta - u^0\|_{L^2(\Omega)} \to 0$, we notice that

$$\lim_{\delta \to 0} \|u^\delta - u^0\|_{L^2(\Omega)} \leq \sup_{\delta \in (0, \delta_0)} \|u^{\delta,\epsilon} - u^\delta\|_{L^2(\Omega)} + \lim_{\delta \to 0} \|u^{\delta,\epsilon} - u^{0,\epsilon}\|_{L^2(\Omega)} + \|u^{0,\epsilon} - u^0\|_{L^2(\Omega)},$$

for any $\epsilon > 0$. Therefore, we only need to show

$$\begin{cases} \lim_{\epsilon \to 0} \sup_{\delta \in (0, \delta_0)} \|u^{\delta,\epsilon} - u^\delta\|_{L^2(\Omega)} = 0, \quad \text{and} \\ \lim_{\epsilon \to 0} \|u^{0,\epsilon} - u^0\|_{L^2(\Omega)} = 0. \end{cases} \tag{2.11}$$

For the first equation in (2.11), we first notice that $\|A^\epsilon - A\|_{C((\Omega \cup \Omega_\delta)^2)} \to 0$ as $\epsilon \to 0$ since $A(\boldsymbol{x}, \boldsymbol{y})$ is uniformly continuous on $\overline{(\Omega \cup \Omega_\delta)^2}$. Now since $u^{\delta,\epsilon}$ and u^δ are solutions to (2.2) with different coefficients and the same right-hand side, we have

$$(A^\epsilon \mathcal{G}[u^{\delta,\epsilon} - u^\delta], \mathcal{G}[v])_{L^2((\Omega \cup \Omega_\delta)^2)} = ((A - A^\epsilon)\mathcal{G}[u^\delta], \mathcal{G}[v])_{L^2((\Omega \cup \Omega_\delta)^2)} =: \langle g^{\delta,\epsilon}, v \rangle,$$

for any $v \in S_\delta(\Omega)$. We can show $\langle g^{\delta,\epsilon}, v \rangle \to 0$ as $\epsilon \to 0$ uniformly independent of δ since

$$\langle g^{\delta,\epsilon}, v \rangle \leq \|A - A^\epsilon\|_{C((\Omega \cup \Omega_\delta)^2)} \|u^\delta\|_{S_\delta(\Omega)} \|v\|_{S_\delta(\Omega)} \leq C\|A - A^\epsilon\|_{C((\Omega \cup \Omega_\delta)^2)} \|v\|_{S_\delta(\Omega)},$$

where we have used $\|u^\delta\|_{S_\delta(\Omega)} \leq C$ from (2.10). Therefore, we have

$$\sup_{\delta \in (0, \delta_0)} \|u^{\delta,\epsilon} - u^\delta\|_{S_\delta(\Omega)} \leq C \sup_{\delta \in (0, \delta_0)} \|g^{\delta,\epsilon}\|_{(S_\delta(\Omega))^*} \leq C\|A - A^\epsilon\|_{C((\Omega \cup \Omega_\delta)^2)} \to 0$$

as $\epsilon \to 0$ and the convergence in L^2 is then implied from the Poincaré inequality. The proof for the second equation in (2.11) is similar by noticing that $\|a^\epsilon - a\|_{C(\Omega)} \to 0$ as $\epsilon \to 0$. $\qquad \square$

Remark 2.3. Notice that here and for the rest of Section 2, we focus on the weak solutions of the nonlocal and local problems, for which no extra regularity assumptions (in the physical space) are needed in terms of well-posedness and convergence. In Section 3, we will discuss the convergence of a meshfree method for the nonlocal problems, which requires stronger regularity assumptions.

Remark 2.4. Although this paper mostly focuses on the "exterior boundary layer" setting because it is more popular in literature [27, 67–72], in some occasions, such as in the local-to-nonlocal volume constraint conversion problem [73, 74], one might find imposing boundary conditions on an interior boundary layer of Ω:

$$\Omega_{-\delta} := \{ \boldsymbol{x} \in \Omega : \text{dist}(\boldsymbol{x}, \partial\Omega) < \delta \}$$

more convenient. With this setting, we define nonlocal boundary conditions $u^D(\boldsymbol{x}) := u^0(\boldsymbol{x})$ on the inner layer of Ω, where u^0 is the local solution, and aim to solve for the solution $u(\boldsymbol{x})$ with $\boldsymbol{x} \in \Omega \backslash \Omega_{-\delta}$. We could also study the convergence of nonlocal solutions to the local limit $u^0(\boldsymbol{x})$ on the whole domain Ω. In fact, in [66], it was shown that with this "interior boundary layer" setting, the nonlocal analytical solution is guaranteed to converge to the local limit. To demonstrate the empirical performance of our proposed approach on both settings, in our first four numerical examples the "exterior boundary layer" setting is applied, while the "interior boundary layer" setting is considered in the last two examples.

2.2. Parametric Nonlocal Diffusion Problem

We now consider the case in which the coefficient A is provided by a random field $A(\boldsymbol{x}, \boldsymbol{y}, \omega)$, where $\omega \in \Omega_p$ and Ω_p is the sample space of a probability space $(\Omega_p, \mathcal{F}, \mathcal{P})$. Here $\mathcal{F}$ is the σ-algebra of subsets of Ω_p and $\mathcal{P}$ is the probability measure. In practice, this random field is usually represented in a "truncated" form using a limited number of random variables (see an example in Section 5.1). Thus, it can be rewritten as $A(\boldsymbol{x}, \boldsymbol{y}, \boldsymbol{\xi})$, where $\boldsymbol{\xi} = (\xi_{(1)}, \xi_{(2)}, \dots, \xi_{(N)})$, N is a positive integer which denotes the dimension of the parametric space, and $\xi_{(i)}$ are random variables. In practice, we often assume they are independent and identically distributed (i.i.d.) random variables. Under this setting, we consider $A(\boldsymbol{x}, \boldsymbol{y}, \boldsymbol{\xi}) : (\Omega \cup \Omega_\delta) \times (\Omega \cup \Omega_\delta) \times \Gamma \to \mathbb{R}$, where Γ is the space of $\boldsymbol{\xi}$ and it is typically called random space or parametric space. Without loss of generality, here we assume that $\Gamma = \prod_{i=1}^{N} \Gamma_i \subset \mathbb{R}^N$ where $\Gamma_i = [-1, 1]$, and the random variable $\boldsymbol{\xi} \in \Gamma$ has a probability density $\rho : \Gamma \to \mathbb{R}^+$. We are interested in solving the family of nonlocal elliptic equations given by

$$\begin{cases} -\mathcal{D}[A(\boldsymbol{x}, \boldsymbol{y}, \boldsymbol{\xi})\mathcal{G}[u]](\boldsymbol{x}) = f(\boldsymbol{x}), & \text{for } \boldsymbol{x} \in \Omega \\ u(\boldsymbol{x}) = u^D(\boldsymbol{x}), & \text{for } \boldsymbol{x} \in \Omega_\delta. \end{cases} \tag{2.12}$$

For each $\boldsymbol{\xi} \in \Gamma$, we assume that $A(\boldsymbol{x}, \boldsymbol{y}, \boldsymbol{\xi})$ is symmetric in its first two variables and $A(\boldsymbol{x}, \boldsymbol{y}, \boldsymbol{\xi}) \in L^\infty((\Omega \cup \Omega_\delta)^2)$. We also assume the uniform ellipticity of the nonlocal problems, i.e.,

$$0 < r \leq A(\boldsymbol{x}, \boldsymbol{y}, \boldsymbol{\xi}) \leq R < \infty, \tag{2.13}$$

for $\boldsymbol{x}, \boldsymbol{y} \in \Omega \cup \Omega_\delta$ and $\boldsymbol{\xi} \in \Gamma$. Therefore the Lax-Milgram theorem ensures the well-posedness of nonlocal problem for each $\boldsymbol{\xi} \in \Gamma$. In addition, in order to consider the limit $\delta \to 0$, we need to assume that for each $\boldsymbol{\xi} \in \Gamma$ and $\boldsymbol{x} \in \Omega \cup \Omega_\delta$,

$$A(\cdot, \cdot, \boldsymbol{\xi}) \in C(\overline{(\Omega \cup \Omega_\delta)^2}) \text{ and } a(\boldsymbol{x}, \boldsymbol{\xi}) := A(\boldsymbol{x}, \boldsymbol{x}, \boldsymbol{\xi}). \tag{2.14}$$

Then we have the corresponding family of local elliptic equation for each $\boldsymbol{\xi} \in \Gamma$:

$$
\begin{cases}
-\nabla \cdot \big(a(\boldsymbol{x}, \boldsymbol{\xi})\nabla(u(\boldsymbol{x}))\big) = f(\boldsymbol{x}), & \text{for } \boldsymbol{x} \in \Omega \\
u(\boldsymbol{x}) = u^D(\boldsymbol{x}), & \text{for } \boldsymbol{x} \in \partial\Omega.
\end{cases}
\tag{2.15}
$$

For each given parameter $\boldsymbol{\xi} \in \Gamma$, we denote the solution to the nonlocal equation (2.12) by $u^\delta(\boldsymbol{x}, \boldsymbol{\xi})$ and the solution to the corresponding local equation (2.15) by $u^0(\boldsymbol{x}, \boldsymbol{\xi})$. A corollary of Theorem 2.2 is that $u^\delta(\boldsymbol{x}, \boldsymbol{\xi})$ converges to $u^0(\boldsymbol{x}, \boldsymbol{\xi})$ in the space $L^2(\Omega) \otimes L^2_\rho(\Gamma)$ as $\delta \to 0$.

Corollary 2.5. *Assume that* $A(\boldsymbol{x}, \boldsymbol{y}, \boldsymbol{\xi})$ *satisfies* (2.13) *and* (2.14), *then we have*

$$
\lim_{\delta \to 0} \|u^\delta - u^0\|_{L^2(\Omega) \otimes L^2_\rho(\Gamma)} = 0.
$$

Proof. For any $\boldsymbol{\xi} \in \Gamma$, and, we know from Theorem 2.2 that $\|u^\delta(\cdot, \boldsymbol{\xi})\|_{S_\delta(\Omega)} \leq C$ for all $\delta \in (0, \delta_0)$ and $\|u^\delta(\cdot, \boldsymbol{\xi}) - u^0(\cdot, \boldsymbol{\xi})\|_{L^2(\Omega)} \to 0$ as $\delta \to 0$. Therefore, it is easy to see that $\|u^\delta(\cdot, \boldsymbol{\xi}) - u^0(\cdot, \boldsymbol{\xi})\|_{L^2(\Omega)} \leq C$ for all $\boldsymbol{\xi} \in \Gamma$ and $\delta \in (0, \delta_0)$. By invoking the dominated convergence theorem, we have

$$
\|u^\delta - u^0\|_{L^2(\Omega) \otimes L^2_\rho(\Gamma)} = \int_\Gamma \|u^\delta(\cdot, \boldsymbol{\xi}) - u^0(\cdot, \boldsymbol{\xi})\|^2_{L^2(\Omega)}\rho(\boldsymbol{\xi})\,d\boldsymbol{\xi} \xrightarrow{\delta \to 0} 0.
$$

$\square$

To discuss the regularity of solutions with respect to the parameter space, we need to assume the existence of a holomorphic extension of $A(\boldsymbol{x}, \boldsymbol{y}, \boldsymbol{\xi})$.

Assumption 2.6 (Holomorphic parameter dependence)**.** The complex continuation of $A(\boldsymbol{x}, \boldsymbol{y}, \boldsymbol{\xi})$, represented as the map $A : \mathbb{C}^N \to L^\infty((\Omega \cup \Omega_\delta)^2)$ is a $L^\infty((\Omega \cup \Omega_\delta)^2)$-valued holomorphic function on $\mathbb{C}^N$.

This condition is easily fulfilled with $A(\boldsymbol{x}, \boldsymbol{y}, \boldsymbol{\xi})$ consisting of polynomials, exponential, sine and cosine functions of the variables $\xi_{(1)}, \xi_{(2)}, \cdots, \xi_{(N)}$. For example, the holomorphic extension exists if $A(\boldsymbol{x}, \boldsymbol{y}, \boldsymbol{\xi}) = \bar{A}(\boldsymbol{x}, \boldsymbol{y}) + \sum_{i=1}^N f_i(\xi_{(i)})\psi_i(\boldsymbol{x}, \boldsymbol{y})$, where $\bar{A} \in L^\infty((\Omega \cup \Omega_\delta)^2)$, $\psi_i \in L^\infty((\Omega \cup \Omega_\delta)^2)$, and f_i is a polynomial, exponential, sine or cosine function $(1 \leq i \leq N)$.

2.2.1. Analytic regularity

In order for the function $u^\delta(\boldsymbol{x}, \boldsymbol{\xi})$ to be uniformly recovered by polynomial expansions in the parameter space, we will show the analyticity of the solution u^δ with respect to the parameterization. By Assumption 2.6, we can extend the definition of $A(\boldsymbol{x}, \boldsymbol{y}, \boldsymbol{\xi})$ to $A(\boldsymbol{x}, \boldsymbol{y}, \hat{\boldsymbol{\xi}})$ where $\hat{\boldsymbol{\xi}}$ belongs to the complex domain

$$
\hat{\Gamma} := \otimes_{1 \leq i \leq N}\{\hat{\xi}_{(i)} \in \mathbb{C} : |\hat{\xi}_{(i)}| \leq 1\}.
$$

Next, we need the complex uniform ellipticity assumption, namely there exists $r_c, R_c \in \mathbb{R}$ such that

$$0 < r_c \leq \text{Re}(A(\boldsymbol{x}, \boldsymbol{y}, \hat{\boldsymbol{\xi}})) \leq |A(\boldsymbol{x}, \boldsymbol{y}, \hat{\boldsymbol{\xi}})| \leq R_c < \infty. \tag{2.16}$$

for $\boldsymbol{x}, \boldsymbol{y} \in \Omega \cup \Omega_\delta$ and $\hat{\boldsymbol{\xi}} \in \hat{\Gamma}$. Therefore the nonlocal problem with the complex coefficient $A(\boldsymbol{x}, \boldsymbol{y}, \hat{\boldsymbol{\xi}})$ is well-posed and the corresponding solution is denoted by $u^\delta(\boldsymbol{x}, \hat{\boldsymbol{\xi}})$. Here we also remark that for the analyticity of solutions to hold, non-affine coefficients may also be used as long as $\boldsymbol{\xi} \mapsto A(\boldsymbol{x}, \boldsymbol{y}, \boldsymbol{\xi})$ possesses an analytic extension to the complex domains and the complex uniform ellipticity condition is satisfied, see related discussion for the local elliptic equations in [75]. We also define the set

$$\mathcal{A} := \{\hat{\boldsymbol{\xi}} \in \mathbb{C}^N : \frac{r_c}{2} < \text{Re}(A(\boldsymbol{x}, \boldsymbol{y}, \hat{\boldsymbol{\xi}})) \leq |A(\boldsymbol{x}, \boldsymbol{y}, \hat{\boldsymbol{\xi}})| < 2R_c\}.$$

So it is clear that the set $\mathcal{A}$ contains $\hat{\Gamma}$.

For the discussions in this Section, we need the complex function spaces. We let $S_\delta(\Omega, \mathbb{C})$ be the space of complex valued functions with norm

$$\|u\|^2_{S_\delta(\Omega, \mathbb{C})} = \int_{\Omega \cup \Omega_\delta} \int_{\Omega \cup \Omega_\delta} \gamma_\delta(|\boldsymbol{y} - \boldsymbol{x}|)|u(\boldsymbol{y}) - u(\boldsymbol{x})|^2 \, d\boldsymbol{y} d\boldsymbol{x},$$

where $|u(\boldsymbol{y}) - u(\boldsymbol{x})|^2$ is understood as $\overline{(u(\boldsymbol{y}) - u(\boldsymbol{x}))}(u(\boldsymbol{y}) - u(\boldsymbol{x}))$ and γ_δ is still the real valued kernel function. $(S_\delta(\Omega, \mathbb{C}))^*$ is the dual space of $S_\delta(\Omega, \mathbb{C})$ equipped with the induced norm. The main result of the this Section is the following theorem on the analyticity of solutions.

Theorem 2.7. *Assume that* $A(\boldsymbol{x}, \boldsymbol{y}, \hat{\boldsymbol{\xi}})$ *satisfies* (2.16), *then the function* $\hat{\boldsymbol{\xi}} \mapsto u(\boldsymbol{x}, \hat{\boldsymbol{\xi}})$ *is holomorphic in an open neighborhood of* $\hat{\Gamma}$.

To prove the theorem, we first need a stability lemma.

Lemma 2.8. *Suppose* u^δ *and* $\tilde{u}^\delta$ *are two solutions of* (2.2) *with the same right-hand side* f *and different coefficients* $A(\boldsymbol{x}, \boldsymbol{y})$ *and* $\tilde{A}(\boldsymbol{x}, \boldsymbol{y})$ *satisfying* (2.3), *then*

$$\|u^\delta - \tilde{u}^\delta\|_{S_\delta(\Omega)} \leq \|A - \tilde{A}\|_{L^\infty((\Omega \cup \Omega_\delta)^2)} \frac{\|f\|_{(S_\delta(\Omega))^*}}{r^2}$$

Proof. Subtracting the variational formulations for u^δ and $\tilde{u}^\delta$, we find that

$$0 = \iint_{(\Omega \cup \Omega_\delta)^2} \left(A\mathcal{G}[u^\delta](\boldsymbol{x}, \boldsymbol{y}) - \tilde{A}\mathcal{G}[\tilde{u}^\delta](\boldsymbol{x}, \boldsymbol{y}) \right) \mathcal{G}[v](\boldsymbol{x}, \boldsymbol{y}) d\boldsymbol{y} d\boldsymbol{x}$$

$$= \iint_{(\Omega \cup \Omega_\delta)^2} A \big(\mathcal{G}[u^\delta](\boldsymbol{x}, \boldsymbol{y}) - \mathcal{G}[\tilde{u}^\delta](\boldsymbol{x}, \boldsymbol{y}) \big) \mathcal{G}[v](\boldsymbol{x}, \boldsymbol{y}) d\boldsymbol{y} d\boldsymbol{x} + \iint_{(\Omega \cup \Omega_\delta)^2} (A - \tilde{A}) \mathcal{G}[\tilde{u}^\delta](\boldsymbol{x}, \boldsymbol{y}) \mathcal{G}[v](\boldsymbol{x}, \boldsymbol{y}) d\boldsymbol{y} d\boldsymbol{x}.$$

13

Therefore $w = u^\delta - \tilde{u}^\delta$ is a solution of

$$\iint_{(\Omega \cup \Omega_\delta)^2} A(\boldsymbol{x}, \boldsymbol{y}) \mathcal{G}[w](\boldsymbol{x}, \boldsymbol{y}) \mathcal{G}[v](\boldsymbol{x}, \boldsymbol{y}) d\boldsymbol{y} d\boldsymbol{x} = \langle l, v \rangle$$

where $\langle l, v \rangle := \iint (\tilde{A} - A) \mathcal{G}[\tilde{u}^\delta] \mathcal{G}[v] d\boldsymbol{y} d\boldsymbol{x}$. So from (2.10) we have

$$\|w\|_{S_\delta(\Omega)} \leq \frac{\|l\|_{(S_\delta(\Omega))^*}}{r} \leq \frac{\|A - \tilde{A}\|_{L^\infty((\Omega \cup \Omega_\delta)^2)} \|\tilde{u}^\delta\|_{S_\delta(\Omega)}}{r} \leq \|A - \tilde{A}\|_{L^\infty((\Omega \cup \Omega_\delta)^2)} \frac{\|f\|_{(S_\delta(\Omega))^*}}{r^2}.$$

$\square$

From the proof of the stability lemma, it is easy to see that similar stability estimate holds when A and $\tilde{A}$ are dependent on the parameter $\boldsymbol{\xi} \in \mathbb{R}^N$ (or $\hat{\boldsymbol{\xi}} \in \mathbb{C}^N$) as long as A (or $\mathrm{Re}A$) and $\tilde{A}$ (or $\mathrm{Re}\tilde{A}$) are bounded below. Now Theorem 2.7 can be proved in a similar way as the its local counterpart in [76, Lemma 2.2].

Proof of Theorem 2.7. For simplicity of notations, sometimes we only write the explicit dependence of functions on the parameter $\hat{\boldsymbol{\xi}}$ in the discussion, although they may also depend on the spatial variables. First, it is easy to see that $\mathcal{A}$ is an open neighborhood of $\hat{\Gamma}$ by the continuity of the maps $\hat{\boldsymbol{\xi}} \mapsto \mathrm{Re}A(\hat{\boldsymbol{\xi}})$ and $\hat{\boldsymbol{\xi}} \mapsto |A(\hat{\boldsymbol{\xi}})|$. Now we will show that for all $\hat{\boldsymbol{\xi}} \in \mathcal{A}$, the function $\hat{\boldsymbol{\xi}} \mapsto u^\delta(\hat{\boldsymbol{\xi}})$ admits a complex derivative $\partial_{\hat{\xi}_{(i)}} u^\delta(\hat{\boldsymbol{\xi}}) \in S_\delta(\Omega, \mathbb{C})$ for $i \in \{1, \cdots, N\}$.

Let $\boldsymbol{e}_i \in \mathbb{R}^N$ be the unit vector in the i-th dimension. For $\hat{h} \in \mathbb{C} \backslash \{0\}$, define the difference quotient function

$$w_{\hat{h}}^\delta(\hat{\boldsymbol{\xi}}) = \frac{u^\delta(\hat{\boldsymbol{\xi}} + \hat{h}\boldsymbol{e}_i) - u^\delta(\hat{\boldsymbol{\xi}})}{\hat{h}} \in S_\delta(\Omega; \mathbb{C}).$$

Since the maps $\hat{\boldsymbol{\xi}} \mapsto \mathrm{Re}A(\hat{\boldsymbol{\xi}})$ and $\hat{\boldsymbol{\xi}} \mapsto |A(\hat{\boldsymbol{\xi}})|$ are continuous, we have the boundedness of $\mathrm{Re}A(\hat{\boldsymbol{\xi}} + \hat{h}\boldsymbol{e}_i)$ and $|A(\hat{\boldsymbol{\xi}} + \hat{h}\boldsymbol{e}_i)|$ for sufficiently small $\hat{h}$. Therefore $w_{\hat{h}}^\delta$ is well-defined for sufficiently small $\hat{h}$. Then for all $v \in S_\delta(\Omega; \mathbb{C})$,

$$\begin{aligned} 0 &= \iint_{(\Omega \cup \Omega_\delta)^2} A(\boldsymbol{x}, \boldsymbol{y}, \hat{\boldsymbol{\xi}} + \hat{h}\boldsymbol{e}_j) \mathcal{G}[u^\delta(\hat{\boldsymbol{\xi}} + \hat{h}\boldsymbol{e}_j)](\boldsymbol{x}, \boldsymbol{y}) \overline{\mathcal{G}[v](\boldsymbol{x}, \boldsymbol{y})} d\boldsymbol{y} d\boldsymbol{x} \\ &\quad - \iint_{(\Omega \cup \Omega_\delta)^2} A(\boldsymbol{x}, \boldsymbol{y}, \hat{\boldsymbol{\xi}}) \mathcal{G}[u^\delta(\hat{\boldsymbol{\xi}})](\boldsymbol{x}, \boldsymbol{y}) \overline{\mathcal{G}[v](\boldsymbol{x}, \boldsymbol{y})} d\boldsymbol{y} d\boldsymbol{x} \\ &= \hat{h} \iint_{(\Omega \cup \Omega_\delta)^2} A(\boldsymbol{x}, \boldsymbol{y}, \hat{\boldsymbol{\xi}}) \mathcal{G}[w_{\hat{h}}^\delta(\hat{\boldsymbol{\xi}})](\boldsymbol{x}, \boldsymbol{y}) \overline{\mathcal{G}[v](\boldsymbol{x}, \boldsymbol{y})} d\boldsymbol{y} d\boldsymbol{x} \\ &\quad + \hat{h} \iint_{(\Omega \cup \Omega_\delta)^2} \psi_i(\boldsymbol{x}, \boldsymbol{y}) \mathcal{G}[u^\delta(\hat{\boldsymbol{\xi}} + \hat{h}\boldsymbol{e}_j)](\boldsymbol{x}, \boldsymbol{y}) \overline{\mathcal{G}[v](\boldsymbol{x}, \boldsymbol{y})} d\boldsymbol{y} d\boldsymbol{x}. \end{aligned}$$

Therefore $w_{\hat{h}}^\delta$ is the unique solution to the variational problem

$$\iint_{(\Omega \cup \Omega_\delta)^2} A(\boldsymbol{x}, \boldsymbol{y}, \hat{\boldsymbol{\xi}}) \mathcal{G}[w_{\hat{h}}^\delta(\hat{\boldsymbol{\xi}})](\boldsymbol{x}, \boldsymbol{y}) \overline{\mathcal{G}[v](\boldsymbol{x}, \boldsymbol{y})} d\boldsymbol{y} d\boldsymbol{x} = \langle l_{\hat{h}}, v \rangle,$$

where $\langle l_{\hat{h}}, v \rangle := \iint_{(\Omega \cup \Omega_\delta)^2} \psi_i(\boldsymbol{x}, \boldsymbol{y}) \mathcal{G}[u^\delta(\hat{\boldsymbol{\xi}} + \hat{h}\boldsymbol{e}_j)](\boldsymbol{x}, \boldsymbol{y}) \overline{\mathcal{G}[v](\boldsymbol{x}, \boldsymbol{y})} d\boldsymbol{y} d\boldsymbol{x}$. One can show that $l_{\hat{h}}$ converges to l_0

14

in $(S_\delta(\Omega;\mathbb{C}))^*$. Indeed, for all $v \in S_\delta(\Omega;\mathbb{C})$,

$$|\langle l_{\hat{h}} - l_0, v\rangle| = \left| \iint_{(\Omega\cup\Omega_\delta)^2} \psi_i(\boldsymbol{x},\boldsymbol{y})\mathcal{G}[u^\delta(\hat{\boldsymbol{\xi}} + \hat{h}\boldsymbol{e}_i) - u^\delta(\hat{\boldsymbol{\xi}})](\boldsymbol{x},\boldsymbol{y})\overline{\mathcal{G}[v](\boldsymbol{x},\boldsymbol{y})}d\boldsymbol{y}d\boldsymbol{x} \right|$$

$$\leq \|\psi_i\|_{L^\infty((\Omega\cup\Omega_\delta)^2)}\|u^\delta(\hat{\boldsymbol{\xi}} + \hat{h}\boldsymbol{e}_i) - u^\delta(\hat{\boldsymbol{\xi}})\|_{S_\delta(\Omega;\mathbb{C})}\|v\|_{S_\delta(\Omega;\mathbb{C})}$$

$$\leq \hat{h}\|\psi_i\|_{L^\infty((\Omega\cup\Omega_\delta)^2)}\frac{\|f\|_{(S_\delta(\Omega;\mathbb{C}))^*}}{(r_c/2)^2}\|v\|_{S_\delta(\Omega;\mathbb{C})},$$

in which the last inequality comes from the stability estimate. Therefore, $w_{\hat{h}}^\delta$ converges in $S_\delta(\Omega;\mathbb{C})$ to w_0^δ, which is the solution to

$$\iint_{(\Omega\cup\Omega_\delta)^2} A(\boldsymbol{x},\boldsymbol{y},\hat{\boldsymbol{\xi}})\mathcal{G}[w_0^\delta(\hat{\boldsymbol{\xi}})](\boldsymbol{x},\boldsymbol{y})\overline{\mathcal{G}[v](\boldsymbol{x},\boldsymbol{y})}d\boldsymbol{y}d\boldsymbol{x} = \langle l_0, v\rangle.$$

Hence $\partial_{\hat{\xi}_{(i)}} u^\delta(\hat{\boldsymbol{\xi}}) = w_0^\delta(\hat{\boldsymbol{\xi}}) \in S_\delta(\Omega;\mathbb{C})$. $\square$

3. Spatial and Stochastic Numerical Methods

Algorithm 1 Overall algorithm for the stochastic nonlocal diffusion problem (2.12)

1: **Offline Stage**:

  1a) For spatial discretization, determine a meshfree grid set $\chi_h = \{\boldsymbol{x}_i\}_{i=1}^M \in \Omega \cup \Omega_\delta$ and calculate the optimization-based quadrature weights $\{\omega_{j,i}\}$ for each $\boldsymbol{x}_i \in \chi_h$ by solving (3.5).

  1b) For probabilistic collocation method, determine the (sparse) collocation points set in the parametric space $\Theta_N = \{\boldsymbol{\xi}_k\}_{k=1}^K \in \Gamma$ and the corresponding quadrature weights μ_k following (3.19).

2: **Online Stage**: Solving for (2.12): For $k = 1, \cdots, K$, do

  2a) Assemble the stiffness matrix $\boldsymbol{Q} = [Q_{(i,j)}]$ such that

$$Q_{ij} = \begin{cases} 2\sum\limits_{\boldsymbol{x}_l \in \chi_h \cap B_\delta(\boldsymbol{x}_i)\setminus\{\boldsymbol{x}_i\}} A(\boldsymbol{x}_i, \boldsymbol{x}_l, \boldsymbol{\xi}_k)\gamma_\delta(|\boldsymbol{x}_i - \boldsymbol{x}_l|)\omega_{l,i}, & \text{if } i = j, \\ -2A(\boldsymbol{x}_i, \boldsymbol{x}_j, \boldsymbol{\xi}_k)\gamma_\delta(|\boldsymbol{x}_i - \boldsymbol{x}_j|)\omega_{j,i}, & \text{if } i \neq j \text{ and } \boldsymbol{x}_j \in B_\delta(\boldsymbol{x}_i), \\ 0, & \text{else}, \end{cases}$$

  and the right-hand-side vector $\boldsymbol{f} = [f(\boldsymbol{x}_i)]_{i=1}^M$.

  2b) Compute the numerical solution $\boldsymbol{u} = [u_h^\delta(\boldsymbol{x}_i, \boldsymbol{\xi}_k)]_{i=1}^M$ for the deterministic problem corresponding to the k-th sample by solving $\boldsymbol{u} = \boldsymbol{Q}^{-1}\boldsymbol{f}$.

3: **Postprocessing Stage**: Generate statistical moments of the random solution following (3.14)-(3.15).

3.1. Spatial: Optimization-Based Meshfree Quadrature Rules

In this section we introduce a strong form of particle discretizations of the deterministic nonlocal diffusion problem introduced in Section 2.1. This approach is based upon the optimization-based quadrature rule developed in [33, 37]. Denoting the numerical solution of (2.2) as u_h^δ, two types of convergence are desired in the developed numerical scheme:

$$\lim_{h\to 0}\left\|u_h^\delta - u^\delta\right\|_{L^2(\Omega)} = 0, \quad \text{and} \quad \lim_{h,\delta\to 0}\left\|u_h^\delta - u^0\right\|_{L^2(\Omega)} = 0. \tag{3.1}$$

15

The first type of convergence indicates that the numerical discretization method is consistent with the nonlocal problem with a fixed δ and $h \to 0$, while the second type shows that the nonlocal numerical solution preserves the correct local limit when $h, \delta \to 0$ simultaneously, or equivalently, the numerical scheme is asymptotically compatible. To maintain an easily scalable implementation, in asymptotic compatibility studies we assume δ to be chosen such that the ratio $\frac{\delta}{h}$ is bound by a constant as $\delta \to 0$, restricting ourselves to the "δ-convergence" scenario [77][1][2]. In this setting, one obtains banded stiffness matrices allowing scalable implementations. We will provide truncation error estimates for the quadrature error convergence rates to the nonlocal analytical solution and the local limit, respectively. In this section, to prove the two types of convergences we would need stronger regularity assumptions on the diffusion coefficient $A(\boldsymbol{x}, \boldsymbol{y})$ as follows:

$$A(\boldsymbol{x}, \boldsymbol{y}) \in C^4(\overline{(\Omega \cup \Omega_\delta)^2}), \ 0 < r \leq A(\boldsymbol{x}, \boldsymbol{y}) \leq R < \infty, \ \text{for } \boldsymbol{x}, \boldsymbol{y} \in \Omega \cup \Omega_\delta, \ \text{and } a(\boldsymbol{x}) = A(\boldsymbol{x}, \boldsymbol{x}). \tag{3.2}$$

3.1.1. Mathematical Formulation and Implementation

Discretizing the whole interaction region $\Omega \cup \Omega_\delta$ by a collection of points $\chi_h = \{\boldsymbol{x}_i\}_{\{i=1,2,\cdots,M\}} \subset \Omega \cup \Omega_\delta$, we aim to solve for the solution $u_{(i)} \approx u(\boldsymbol{x}_i)$ on all $\boldsymbol{x}_i \in \chi_h$. Although the method can be applied to more general grids, for analysis we require χ_h to be a uniform Cartesian grid:

$$\chi_h := \{(k_{(1)}h, \cdots, k_{(d)}h) | \boldsymbol{k} = (k_{(i)}, \cdots, k_{(d)}) \in \mathbb{Z}^d\} \cap (\Omega \cup \Omega_\delta).$$

Here h is the spatial grid size. For the deterministic nonlocal diffusion model (2.2) we pursue a discretization through the following one point quadrature rule at χ_h [78]:

$$-(\mathcal{L}_h^\delta u)_{(i)} := -2 \sum_{\boldsymbol{x}_j \in \chi_h \cap B_\delta(\boldsymbol{x}_i) \setminus \{\boldsymbol{x}_i\}} A(\boldsymbol{x}_i, \boldsymbol{x}_j) \gamma_\delta(|\boldsymbol{x}_i - \boldsymbol{x}_j|)(u_{(j)} - u_{(i)})\omega_{j,i} = f(\boldsymbol{x}_i), \qquad \text{for } \boldsymbol{x}_i \in \chi_h \cap \Omega,$$

$$u_{(i)} = u^D(\boldsymbol{x}_i), \qquad\qquad\qquad\qquad\qquad\qquad\qquad\qquad\qquad\qquad\qquad \text{for } \boldsymbol{x}_i \in \chi_h \cap \Omega_\delta,$$

$$\tag{3.3}$$

where we specify $\{\omega_{j,i}\}$ as a to-be-determined collection of quadrature weights admitting interpretation as a measure associated with each collocation point $\boldsymbol{x}_i$. Note that although we only solve for $u_{(i)}$ on grid points in χ_h, we will denote the numerical solution u_h^δ of the above nonlocal problem as the piecewise constant interpolation of $u_{(i)}$.

We use an optimization-based approach to define these weights extending previous work [33, 37], constructed to ensure consistency guarantees. Specifically, we seek quadrature weights for integrals supported

---

[1]In some literature it is also denoted as the "M-convergence", see, e.g., [37].
[2]Typically in the literature a scheme is termed as asymptotically compatible (AC) if it recovers the classical solution for any $\delta, h \to 0$. Here we abuse the definition slightly and only require the δ-convergence.

on balls of the form

$$I[q] := \int_{B_\delta(\boldsymbol{x_i})} q(\boldsymbol{x_i}, \boldsymbol{y}) d\boldsymbol{y} \approx I_h[q] := \sum_{\boldsymbol{x_j} \in \chi_h \cap B_\delta(\boldsymbol{x_i}) \backslash \{\boldsymbol{x_i}\}} q(\boldsymbol{x_i}, \boldsymbol{x_j}) \omega_{j,i} \tag{3.4}$$

where we include the subscript i in $\{\omega_{j,i}\}$ to denote that we seek a different family of quadrature weights for different subdomains $B_\delta(\boldsymbol{x_i})$. Denoting $\boldsymbol{P}_m(\mathbb{R}^d)$ as the space of m-th order polynomials, we obtain these weights from the following optimization problem

$$\operatorname*{argmin}_{\{\omega_{j,i}\}} \sum_{\boldsymbol{x_j} \in \chi_h \cap B_\delta(\boldsymbol{x_i}) \backslash \{\boldsymbol{x_i}\}} \frac{\omega_{j,i}^2 W(|\boldsymbol{x_j} - \boldsymbol{x_i}|)}{2} \quad \text{such that,} \quad I_h[q] = I[q] \quad \forall q \in \boldsymbol{V}_{h,\boldsymbol{x_i}} \tag{3.5}$$

where $\boldsymbol{V}_{h,\boldsymbol{x_i}} = \boldsymbol{S}_{\gamma_\delta,\boldsymbol{x_i}} := \{q = p(\boldsymbol{y} - \boldsymbol{x_i})\gamma_\delta(|\boldsymbol{x_i} - \boldsymbol{y}|) \,|\, p \in \boldsymbol{P}_3(\mathbb{R}^d)\}$ denotes the space of functions which should be integrated exactly. Note that when $p(\boldsymbol{x}) = const$, we have $q(\boldsymbol{x}, \boldsymbol{y}) = \gamma_\delta(|\boldsymbol{x} - \boldsymbol{y}|)$. Therefore, reproducing this function requires the kernel function γ_δ to be integrable, or equivalently, $s < d$. $W(r)$ is a radially symmetric positive weight function supported in $B_\delta(\boldsymbol{0})$. Following the discussions in [28], we take $W(r) = \gamma_\delta(r)$. In [33], this particular choice of reproducing space provides the minimal reproducing set to achieve the optimal $O(\delta^2)$ asymptotic convergence rate in nonlocal problems with homogeneous diffusion coefficient[3]. We note that provided the quadrature points are unisolvent over the desired reproducing space, (3.5) may be proven to have a solution by interpreting it as a generalized moving least squares (GMLS) problem [28]. For certain choices of $\boldsymbol{V}_{h,\boldsymbol{x_i}}$, such as m-th order polynomials, unisolvency holds under the following assumptions: the domain Ω satisfies a cone condition, the pointset $\chi_h \cap B_\delta(\boldsymbol{x_i})$ is quasi-uniform, and h/δ is sufficiently small (see, e.g., [79, 80, Chapter 4]).

For each $\boldsymbol{x_i} \in \chi_h \cap \Omega$, we denote the set of its interacting neighbor points as $\{\boldsymbol{x_j}\}_{j=1,\cdots,M_i} = \chi_h \cap B_\delta(\boldsymbol{x_i}) \backslash \{\boldsymbol{x_i}\}$ and the corresponding quadrature weights in a size M_i vector, denoted as $\boldsymbol{\omega} = [\omega_{1,i}, \cdots, \omega_{M_i,i}]^T$. With the Lagrange multiplier method, quadrature weights may be obtained from (3.5) by solving the saddle-point problem for each $\boldsymbol{x_i}$,

$$\begin{bmatrix} \boldsymbol{W} & \boldsymbol{H}^\intercal \\ \boldsymbol{H} & \boldsymbol{0} \end{bmatrix} \begin{bmatrix} \boldsymbol{\omega} \\ \boldsymbol{\lambda} \end{bmatrix} = \begin{bmatrix} \boldsymbol{0} \\ \boldsymbol{g} \end{bmatrix}, \tag{3.6}$$

where $\boldsymbol{W}$ is an $M_i \times M_i$ diagonal matrix with $\boldsymbol{W}_{kk} = \gamma_\delta(|\boldsymbol{x_k} - \boldsymbol{x_i}|)$, $\boldsymbol{\lambda} \in \mathbb{R}^{dim(\boldsymbol{V}_{h,\boldsymbol{x_i}})}$ is a set of Lagrange multipliers used to enforce reproducability, $\boldsymbol{H} = [H_{(\alpha,j)}] \in \mathbb{R}^{M_i \times dim(\boldsymbol{V}_{h,\boldsymbol{x_i}})}$ consists of the reproducing set evaluated at each quadrature point (i.e. $H_{(\alpha,j)} = p_\alpha(\boldsymbol{x_j})$, for all $p_\alpha \in \boldsymbol{V}_{h,\boldsymbol{x_i}}$), and $\boldsymbol{g} = [g_{(\alpha)}] \in \mathbb{R}^{dim(\boldsymbol{V}_{h,\boldsymbol{x_i}})}$ consists of the integral of each function in the reproducing set over the ball such that $g_{(\alpha)} = I[p_\alpha]$. In particular, when considering $\boldsymbol{V}_{h,\boldsymbol{x_i}} = \boldsymbol{S}_{\gamma_\delta,\boldsymbol{x_i}}$, and denoting $\gamma_{ji}^\delta := \gamma_\delta(|\boldsymbol{x_i} - \boldsymbol{x_j}|)$, we then have $\boldsymbol{g} = [g_{(\boldsymbol{\beta})}]^\intercal$,

---

[3]Notice that in [33], besides the weights $\omega_{j,i}$ considered here, one also solves for an additional associated weight $\omega_{i,i}$. However, since $u_{(i)} - u_{(i)} = 0$ in (3.3), in the current work we simplify the formulation and only solve for $\omega_{j,i}$ with $\boldsymbol{x_j} \neq \boldsymbol{x_i}$. When assigning $\omega_{i,i} := \text{Volume}(B_\delta(\boldsymbol{0})) - \sum_{\boldsymbol{x_j} \in \chi_h \cap B_\delta(\boldsymbol{x_i}) \backslash \{\boldsymbol{x_i}\}} \omega_{j,i}$ the quadrature rule with minimal reproducing function space $\boldsymbol{V}_{h,\boldsymbol{x_i}} = P_0(\mathbb{R}^d) \cup \boldsymbol{S}_{\gamma_\delta,\boldsymbol{x_i}}$ in [33] is in fact equivalent to the quadrature rule with reproducing function space $\boldsymbol{V}_{h,\boldsymbol{x_i}} = \boldsymbol{S}_{\gamma_\delta,\boldsymbol{x_i}}$ considered here.

$\boldsymbol{H} = [H_{(\boldsymbol{\beta},j)}]$ for $j = 1, \cdots, M_i$ and $\boldsymbol{\beta} = (\beta_{(1)}, \cdots, \beta_{(d)}) \in \mathbb{N}^d$, $0 \leq |\boldsymbol{\beta}|_{l_1} \leq 3$, where

$$g_{(\boldsymbol{\beta})} = g_{(\beta_{(1)}, \cdots, \beta_{(d)})} = \int_{B_\delta(\boldsymbol{0})} \gamma_\delta(|\boldsymbol{x}_i - \boldsymbol{y}|)(\boldsymbol{y} - \boldsymbol{x}_i)_{(1)}^{\beta_{(1)}} \cdots (\boldsymbol{y} - \boldsymbol{x}_i)_{(d)}^{\beta_{(d)}} d\boldsymbol{y} \quad \text{for } |\boldsymbol{\beta}|_{l_1} \neq 0,$$

$$H_{(\boldsymbol{\beta},j)} = \gamma_{ji}^\delta \cdot (\boldsymbol{x}_j - \boldsymbol{x}_i)_{(1)}^{\beta_{(1)}} \cdots (\boldsymbol{x}_j - \boldsymbol{x}_i)_{(d)}^{\beta_{(d)}}.$$

By eliminating the constraints, the quadrature weights may be obtained by solving

$$\boldsymbol{\omega} = \boldsymbol{W}^{-1} \boldsymbol{H}^{\mathsf{T}} [\boldsymbol{H} \boldsymbol{W}^{-1} \boldsymbol{H}^{\mathsf{T}}]^{-1} \boldsymbol{g}, \tag{3.7}$$

where $\boldsymbol{H}\boldsymbol{W}^{-1}\boldsymbol{H}^{\mathsf{T}} = [m_{(\boldsymbol{\beta},\boldsymbol{\theta})}]$ for $\boldsymbol{\beta} = (\beta_{(1)}, \cdots, \beta_{(d)})$, $\boldsymbol{\theta} = (\theta_{(1)}, \cdots, \theta_{(d)})$, and $0 \leq |\boldsymbol{\beta}|_{l_1} \le 3$, $0 \le |\boldsymbol{\theta}|_{l_1} \leq 3$ satisfying

$$m_{(\boldsymbol{\beta},\boldsymbol{\theta})} = m_{(\boldsymbol{\theta},\boldsymbol{\beta})}, \quad m_{(\boldsymbol{\beta},\boldsymbol{\theta})} = \sum_{j=1}^{M_i} \gamma_{ji}^\delta (\boldsymbol{x}_j - \boldsymbol{x}_i)_{(1)}^{\beta_{(1)}+\theta_{(1)}} \cdots (\boldsymbol{x}_j - \boldsymbol{x}_i)_{(d)}^{\beta_{(d)}+\theta_{(d)}}.$$

For problems where the reproducing constraints are redundant, $[\boldsymbol{H}\boldsymbol{W}^{-1}\boldsymbol{H}^{\mathsf{T}}]^{-1}$ may be replaced by the pseudo-inverse.

3.1.2. Stability and Convergence Analysis

To provide the stability proof of our method, we first show that the quadrature weights are all positive. To guarantee the unisolvency of the optimization problem (3.5) (see, e.g., [80, Chapter 4]), in the following we assume that $h < C_{sol}\delta$ for a given constant $C_{sol} < 1$ in all cases. Moreover, we also assume that δ is bounded by a generic constant, i.e., $\delta \leq C$.

Lemma 3.1. *Consider a kernel γ_δ defined in (2.1) with $s < d$. For a given $\boldsymbol{x}_i$ and $h < C_{sol}\delta$, quadrature weights obtained from (3.5) with the choice of $V_{h,\boldsymbol{x}_i} = \boldsymbol{S}_{\gamma_\delta,\boldsymbol{x}_i}$ satisfy:*

$$|\omega_{j,i} - h^d| \leq Ch^d(h/\delta)^{\min(1,d-s)}, \tag{3.8}$$

where C is a constant independent of h and δ.

Proof. With the symmetry property of γ_δ and the uniform Cartesian grid assumption, we note that $g_{(\boldsymbol{\beta})} = 0$ if one of the components of $\boldsymbol{\beta}$ is an odd number, and $m_{(\boldsymbol{\beta},\boldsymbol{\theta})} = 0$ if one of the components of $\boldsymbol{\beta} + \boldsymbol{\theta}$ is an odd number. Moreover, $g_{(\boldsymbol{\beta})} = g_{(\tilde{\boldsymbol{\beta}})}$ if $\tilde{\boldsymbol{\beta}}$ is a reordering of $\boldsymbol{\beta}$, and $m_{(\boldsymbol{\beta},\boldsymbol{\theta})} = m_{(\tilde{\boldsymbol{\beta}},\tilde{\boldsymbol{\theta}})}$ if $\tilde{\boldsymbol{\beta}} + \tilde{\boldsymbol{\theta}}$ is a reordering of $\boldsymbol{\beta} + \boldsymbol{\theta}$. Denote $\boldsymbol{b} = [\boldsymbol{H}\boldsymbol{W}^{-1}\boldsymbol{H}^{\mathsf{T}}]^{-1}\boldsymbol{g}$, we then have $b_{(\boldsymbol{\beta})} = 0$ unless $|\boldsymbol{\beta}|_{l_1} = 0$ or $|\boldsymbol{\beta}|_{l_1} = 2$ with only one nonzero entry $\beta_k = 2$ for some $k \in \{1, \cdots, d\}$. With the symmetry properties of $g_{(\boldsymbol{\beta})}$ and $m_{(\boldsymbol{\beta},\boldsymbol{\theta})}$, we notice that $b_{(\boldsymbol{\beta})} = b_{(\tilde{\boldsymbol{\beta}})}$ if $\tilde{\boldsymbol{\beta}}$ is a reordering of $\boldsymbol{\beta}$. Therefore, we may denote $b_{(0,\cdots,0)} := b_0$, $b_{(2,0,\cdots,0)} = b_{(0,2,\cdots,0)} = \cdots = b_{(0,\cdots,0,2)} := b_2$,

and b_0, b_2 satisfy:

$$\sum_{j=1}^{M_i} \gamma_{ji}^\delta b_0 + \left[\sum_{j=1}^{M_i}\sum_{k=1}^{d} \gamma_{ji}^\delta (\boldsymbol{x}_j - \boldsymbol{x}_i)_{(k)}^2\right] \cdot b_2 = \int_{B_\delta(\mathbf{0})} \gamma_\delta(|\boldsymbol{y}|) d\boldsymbol{y},$$

$$\left[\sum_{j=1}^{M_i} \gamma_{ji}^\delta (\boldsymbol{x}_j - \boldsymbol{x}_i)_{(1)}^2\right] b_0 + \left[\sum_{j=1}^{M_i} \gamma_{ji}^\delta (\boldsymbol{x}_j - \boldsymbol{x}_i)_{(1)}^2 \sum_{k=1}^{d} (\boldsymbol{x}_j - \boldsymbol{x}_i)_{(k)}^2\right] \cdot b_2 = \int_{B_\delta(\mathbf{0})} \gamma_\delta(|\boldsymbol{y}|) \boldsymbol{y}_{(1)}^2 d\boldsymbol{y}.$$

Notice that $s < d$ and we now compare the quadrature rule with the Riemann sum estimates for integrals. Denoting that $\hat{h} := h/\delta$, $\hat{\boldsymbol{x}}_j := \boldsymbol{x}_j/\delta$, $\hat{\boldsymbol{y}} := \boldsymbol{y}/\delta$ and $\hat{\gamma}_{ji}^1 := \frac{D_0}{|\hat{\boldsymbol{x}}_j - \hat{\boldsymbol{x}}_i|^s}$, we obtain

$$\left|\sum_{j=1}^{M_i} \gamma_{ji}^\delta h^d - \int_{B_\delta(\mathbf{0})} \gamma_\delta(|\boldsymbol{y}|)d\boldsymbol{y}\right| = \left|\sum_{j=1}^{M_i} \hat{\gamma}_{ji}^1 \hat{h}^d \delta^{-2} - \int_{B_1(\mathbf{0})} \gamma_1(|\hat{\boldsymbol{y}}|)\delta^{-2} d\hat{\boldsymbol{y}}\right|$$

$$\le C\delta^{-2} \int_{B_{\sqrt{d}\hat{h}}(\mathbf{0})} |\hat{\boldsymbol{y}}|^{-s} d\hat{\boldsymbol{y}} + C\delta^{-2}\hat{h} \int_{B_1(\mathbf{0})\backslash B_{\hat{h}}(\mathbf{0})} |\hat{\boldsymbol{y}}|^{-s-1} d\hat{\boldsymbol{y}} \le C\delta^{-2}(\hat{h}^{d-s} + \hat{h}) \le C\delta^{-2}((h/\delta)^{d-s} + h/\delta),$$

$$\left|h^d \sum_{j=1}^{M_i} \gamma_{ji}^\delta (\boldsymbol{x}_j - \boldsymbol{x}_i)_{(1)}^2 - \int_{B_\delta(\mathbf{0})} \gamma_\delta(|\boldsymbol{y}|)\boldsymbol{y}_{(1)}^2 d\boldsymbol{y}\right| = \left|\hat{h}^d \sum_{j=1}^{M_i} \hat{\gamma}_{ji}^1 (\hat{\boldsymbol{x}}_j - \hat{\boldsymbol{x}}_i)_{(1)}^2 - \int_{B_1(\mathbf{0})} \gamma_1(|\hat{\boldsymbol{y}}|)\hat{\boldsymbol{y}}_{(1)}^2 d\hat{\boldsymbol{y}}\right|$$

$$\le C \int_{B_{\sqrt{d}\hat{h}}(\mathbf{0})} |\hat{\boldsymbol{y}}|^{2-s} d\hat{\boldsymbol{y}} + C\hat{h} = C(\hat{h}^{d+2-s} + \hat{h}) \le C\delta^{-1}h,$$

$$\left|h^d \sum_{j=1}^{M_i} \gamma_{ji}^\delta (\boldsymbol{x}_j - \boldsymbol{x}_i)_{(1)}^2 \sum_{k=1}^{d}(\boldsymbol{x}_j - \boldsymbol{x}_i)_{(k)}^2 - \int_{B_\delta(\mathbf{0})} \gamma_\delta(|\boldsymbol{y}|)|\boldsymbol{y}|^2 \boldsymbol{y}_{(1)}^2 d\boldsymbol{y}\right|$$

$$= \delta^2 \left|\hat{h}^d \sum_{j=1}^{M_i} \hat{\gamma}_{ji}^1 (\hat{\boldsymbol{x}}_j - \hat{\boldsymbol{x}}_i)_{(1)}^2 \sum_{k=1}^{d}(\hat{\boldsymbol{x}}_j - \hat{\boldsymbol{x}}_i)_{(k)}^2 - \int_{B_1(\mathbf{0})} \gamma_1(|\hat{\boldsymbol{y}}|)|\hat{\boldsymbol{y}}|^2 \hat{\boldsymbol{y}}_{(1)}^2 d\hat{\boldsymbol{y}}\right|$$

$$\le C\delta^2 \int_{B_{\sqrt{d}\hat{h}}(\mathbf{0})} |\hat{\boldsymbol{y}}|^{4-s} d\hat{\boldsymbol{y}} + C\delta^2\hat{h} \le C(\hat{h}^{d+4-s} + \hat{h}) \le C\delta h,$$

where $B_{\sqrt{d}\hat{h}}(\mathbf{0})$ is a sphere covering the origin point and the singularity on it. Note here we don't have an associated weight $\omega_{i,i}^\delta$, and the errors of integrals in the (hyper)cube containing the origin point with size h^d were estimated separately. $B_{\sqrt{d}\hat{h}}$ is then chosen as a sphere to contain this (hyper)cube. We obtain $b_0 = h^d + h^d O((h/\delta)^{\min(1,d-s)})$, $b_2 = h^d\delta^{-2}O((h/\delta)^{\min(1,d-s)})$, and $\boldsymbol{\omega} = \boldsymbol{W}^{-1}\boldsymbol{H}^\intercal \boldsymbol{b} = h^d \mathbf{1} + O(h^{\min(d+1,2d-s)})\mathbf{1}$, where $\mathbf{1}$ is a size M_i vector with all elements equal 1.

$\square$

From the above lemma and [80], we can see that there exists a constant $C < 1$ which is independent of δ, such that for all $h < C\delta$ unisolvency holds for the optimization problem (3.5) and we have $\omega_{j,i} > 0$. In the following we will denote this constant as C_{pos} and generally require $h < C_{pos}\delta$. Note that the uniform grid assumption and the symmetry property in Lemma 3.1 also yields $\omega_{j,i} = \omega_{i,j}$. Consider A satisfying the conditions in (2.3) and (2.8) and γ_δ satisfying the conditions in Lemma 3.1, we obtain the discrete maximum principle for $\mathcal{L}_h^\delta$ and the well-poseness property of the discretized nonlocal diffusion problem (3.3):

Lemma 3.2 (Discrete Maximum/Minimum Principle). *For $h \leq C_{pos}\delta$, let v_h be a function on χ_h satisfying $\mathcal{L}_h^\delta v_h \geq 0$ on $\chi_h \cap \Omega$, then $\max\limits_{\chi_h \cap \Omega} v_h \leq \max\limits_{\chi_h \cap \Omega_\delta} v_h$.*

Proof. Assume that $\max\limits_{\chi_h \cap \Omega} v_h \geq \max\limits_{\chi_h \cap \Omega_\delta} v_h$ and $v_h(\boldsymbol{x}_i) = \max\limits_{\chi_h \cap \Omega} v_h$, then

$$0 \geq -\mathcal{L}_h^\delta v_h(\boldsymbol{x}_i) = -2 \sum_{\boldsymbol{x}_j \in \chi_h \cap B_\delta(\boldsymbol{x}_i) \setminus \{\boldsymbol{x}_i\}} A(\boldsymbol{x}_i, \boldsymbol{x}_j) \gamma_\delta(|\boldsymbol{x}_i - \boldsymbol{x}_j|) \omega_{j,i}(v_h(\boldsymbol{x}_j) - v_h(\boldsymbol{x}_i)) \geq 0.$$

Therefore, we have $v_h(\boldsymbol{x}_j) = v_h(\boldsymbol{x}_i) = \max\limits_{\chi_h \cap \Omega} v_h$ for all $\boldsymbol{x}_j \in B_\delta(\boldsymbol{x}_i)$. Applying the same argument to $\boldsymbol{x}_j \in B_\delta(\boldsymbol{x}_i)$ in Ω and to their neighbors, one obtains that v_h is a constant on χ_h and therefore $\max\limits_{\chi_h \cap \Omega} v_h = \max\limits_{\chi_h \cap \Omega_\delta} v_h$. $\qquad\square$

With the discrete maximum principle, the discretized nonlocal diffusion problem (3.?) is therefore well-posed, i.e., there exists a unique solution to the discretized nonlocal diffusion problem (3.?). We now consider the accuracy of the quadrature rule. In the following, we first present the truncation error estimate of the meshfree discretization for the nonlocal diffusion problem with fixed δ:

Lemma 3.3. *Consider a kernel γ_δ satisfying the conditions in Lemma ?, a diffusion coefficient function A satisfying the conditions in (3.2), $u(\boldsymbol{x}) \in C^1(\overline{\Omega \cup \Omega_\delta})$, and a fixed δ. Then for $h < C_{pos}\delta$, quadrature weights obtained from (3.5) with the choice of $\boldsymbol{V}_{h,\boldsymbol{x}_i} = \boldsymbol{S}_{\gamma,\boldsymbol{x}_i}$ satisfy the following pointwise error estimate, with $C(\delta) > 0$ being a constant independent of h that may depend on δ.*

$$\max_{\boldsymbol{x}_i \in \chi_h \cap \Omega} \left| \mathcal{L}^\delta[u](\boldsymbol{x}_i) - \mathcal{L}_h^\delta[u](\boldsymbol{x}_i) \right| \leq C(\delta) h^{\min(1, d-s)}. \tag{3.9}$$

Proof. We note that

$$\sum_{j=1}^{M_i} |A(\boldsymbol{x}_i, \boldsymbol{x}_j) \gamma_\delta(|\boldsymbol{x}_i - \boldsymbol{x}_j|)(u(\boldsymbol{x}_j) - u(\boldsymbol{x}_i))| h^{\min(d+1, 2d-s)} \leq C(\delta) \sum_{j=1}^{M_i} |\boldsymbol{x}_i - \boldsymbol{x}_j|^{1-s} h^{\min(d+1, 2d-s)}$$

$$\leq C(\delta) \int_{B_\delta(\boldsymbol{0})} |\boldsymbol{y}|^{1-s} d\boldsymbol{y} \, h^{\min(1, d-s)} \leq C(\delta) h^{\min(1, d-s)}.$$

On the other hand, let $C(\boldsymbol{x}_j)$ denote the (hyper)cubic of size h^d centered at $\boldsymbol{x}_j$, we have the error estimate

of the Riemann sum formulation as:

$$\left| \int_{B_\delta(\boldsymbol{x}_i)} A(\boldsymbol{x}_i, \boldsymbol{y}) \gamma_\delta(|\boldsymbol{x}_i - \boldsymbol{y}|)(u(\boldsymbol{y}) - u(\boldsymbol{x}_i)) \, d\boldsymbol{y} - \sum_{j=1}^{M_i} A(\boldsymbol{x}_i, \boldsymbol{x}_j) \gamma_\delta(|\boldsymbol{x}_i - \boldsymbol{x}_j|)(u(\boldsymbol{x}_j) - u(\boldsymbol{x}_i)) h^d \right|$$

$$\leq C(\delta)h + C(\delta) \int_{B_{\sqrt{d}h}(\boldsymbol{0})} |\boldsymbol{y}|^{1-s} d\boldsymbol{y}$$

$$+ \sum_{j=1}^{M_i} \left| \int_{G(\boldsymbol{x}_j)} A(\boldsymbol{x}_i, \boldsymbol{y}) \gamma_\delta(|\boldsymbol{x}_i - \boldsymbol{y}|)(u(\boldsymbol{y}) - u(\boldsymbol{x}_i)) \, d\boldsymbol{y} - A(\boldsymbol{x}_i, \boldsymbol{x}_j) \gamma_\delta(|\boldsymbol{x}_i - \boldsymbol{x}_j|)(u(\boldsymbol{x}_j) - u(\boldsymbol{x}_i)) h^d \right|$$

$$\leq C(\delta)(h + h^{d-s+1}) + C(\delta) \sum_{j=1}^{M_i} h^{d+1} \max_{\boldsymbol{z} \in G(\boldsymbol{x}_j)} |\nabla_{\boldsymbol{y}}(A(\boldsymbol{x}_i, \boldsymbol{z})(u(\boldsymbol{z}) - u(\boldsymbol{x}_i))\gamma_\delta(|\boldsymbol{x}_i - \boldsymbol{z}|))|$$

$$\leq C(\delta)h + C(\delta) \sum_{j=1}^{M_i} h^{d+1} \left(\max_{\boldsymbol{z} \in G(\boldsymbol{x}_j)} |(u(\boldsymbol{z}) - u(\boldsymbol{x}_i))\nabla_{\boldsymbol{y}}\gamma_\delta(|\boldsymbol{x}_i - \boldsymbol{z}|)| \right.$$

$$\left. + \max_{\boldsymbol{z} \in G(\boldsymbol{x}_j)} \gamma_\delta(|\boldsymbol{x}_i - \boldsymbol{z}|)|\nabla_{\boldsymbol{y}}(A(\boldsymbol{x}_i, \boldsymbol{z})(u(\boldsymbol{z}) - u(\boldsymbol{x}_i)))| \right)$$

$$\leq C(\delta)h + C(\delta) \sum_{j=1}^{M_i} h^{d+1} \left(\max_{\boldsymbol{z} \in G(\boldsymbol{x}_j)} |\boldsymbol{x}_i - \boldsymbol{z}|^{-s} \right) \leq C(\delta)h + C(\delta)h \int_{B_\delta(\boldsymbol{0})} |\boldsymbol{y}|^{-s} d\boldsymbol{y} \leq C(\delta)h$$

where $|\nabla_{\boldsymbol{y}} a(\boldsymbol{x}, \boldsymbol{y})|$ denotes the maximum component of the first order partial derivatives with respect to $\boldsymbol{y}$. Therefore, substituting (3.8) into (3.3) yields

$$\left| \mathcal{L}^\delta[u](\boldsymbol{x}_i) - \mathcal{L}_h^\delta[u](\boldsymbol{x}_i) \right|$$

$$= \left| \int_{B_\delta(\boldsymbol{x}_i)} A(\boldsymbol{x}_i, \boldsymbol{y}) \gamma_\delta(|\boldsymbol{x}_i - \boldsymbol{y}|) u(\boldsymbol{y}) \, d\boldsymbol{y} - \sum_{j=1}^{M_i} A(\boldsymbol{x}_i, \boldsymbol{x}_j) \gamma_\delta(|\boldsymbol{x}_i - \boldsymbol{x}_j|) u(\boldsymbol{x}_j) h^d \right| + O(h^{\min(1, d-s)})$$

$$\leq C(\delta) h^{\min(1, d-s)}.$$

Note here the constant $C(\delta)$ is independent of h but may depend on δ. $\qquad \square$

To prove the asymptotic compatibility, we need the truncation error estimate for convergence to the local limit. In [33, Theorem 2.1], the authors have shown that for a sufficiently smooth u, the quadrature weights obtained from (3.5) with the choice of $\boldsymbol{V}_{h, \boldsymbol{x}_i} = \boldsymbol{S}_{\gamma_\delta, \boldsymbol{x}_i}$ provides an $O(\delta^2)$ pointwise error bound for the integral approximation of $2 \int_{B_\delta(\boldsymbol{x}_i)} \gamma_\delta(|\boldsymbol{x}_i - \boldsymbol{y}|)(u(\boldsymbol{y}) - u(\boldsymbol{x}_i)) \, d\boldsymbol{y}$ when the ratio h/δ is fixed. We can easily extend this error estimate to a nonlocal diffusion operator with heterogeneous diffusion coefficient:

Lemma 3.4. *Consider a kernel γ_δ satisfying the conditions in Lemma 3.1, a diffusion coefficient function A satisfying the conditions in (3.2), $u(\boldsymbol{x}) \in C^4(\overline{\Omega \cup \Omega_\delta})$, and fixed ratio $h/\delta < C_{pos}$. Quadrature weights obtained from (3.5) with the choice of $\boldsymbol{V}_{h, \boldsymbol{x}_i} = \boldsymbol{S}_{\gamma_\delta, \boldsymbol{x}_i}$ satisfy the following pointwise error estimate, with $C > 0$ independent of δ and h:*

$$\max_{\boldsymbol{x}_i \in \boldsymbol{V}_{h, \boldsymbol{x}_i}} \left| \mathcal{L}^\delta[u](\boldsymbol{x}_i) - \mathcal{L}_h^\delta[u](\boldsymbol{x}_i) \right| \leq C \|u\|_{C^4(\overline{\Omega \cup \Omega_\delta})} \delta^2,$$

where $||u||_{C^k(\overline{\Omega \cup \Omega_\delta})} := \max\limits_{\boldsymbol{x} \in \overline{\Omega \cup \Omega_\delta}} \max\limits_{|\boldsymbol{\beta}|=4} \left| D^{\boldsymbol{\beta}} u(\boldsymbol{x}) \right|.$

Proof. Note that for a given $\boldsymbol{x}$ we consider the estimate of $A(\boldsymbol{x}, \boldsymbol{y}) u(\boldsymbol{x}) \in C^4$ and $A(\boldsymbol{x}, \boldsymbol{y}) u(\boldsymbol{y}) \in C^4$, the following truncation estimate is obtained immediately from [33, Theorem 2.1]:

$$\max_{\boldsymbol{x}_i \in \chi_h \cap \Omega} \left| 2 \int_{B_\delta(\boldsymbol{x}_i)} \frac{A(\boldsymbol{x}_i, \boldsymbol{y}) D_0}{|\boldsymbol{x}_i - \boldsymbol{y}|^s} (u(\boldsymbol{y}) - u(\boldsymbol{x}_i)) \, d\boldsymbol{y} \right.$$

$$\left. -2 \sum_{\boldsymbol{x}_j \in \chi_h \cap B_\delta(\boldsymbol{x}_i) \backslash \{\boldsymbol{x}_i\}} \omega_{j,i} \frac{A(\boldsymbol{x}_i, \boldsymbol{x}_j) D_0}{|\boldsymbol{x}_i - \boldsymbol{x}_j|^s} (u(\boldsymbol{x}_j) - u(\boldsymbol{x}_i)) \right| \leq C ||u||_{C^4(\overline{\Omega \cup \Omega_\delta})} \delta^{4-s+d}.$$

And the proof is finished by taking $\gamma_\delta(|\boldsymbol{x} - \boldsymbol{y}|) = \frac{D_0}{\delta^{d+2-s}|\boldsymbol{x}_i - \boldsymbol{y}|^s}$ as stated in (2.1). $\qquad\square$

From the derivation of Theorem 2.2, one can see that $\left| \mathcal{L}^0[u](\boldsymbol{x}_i) - \mathcal{L}^\delta[u](\boldsymbol{x}_i) \right| \leq C ||u||_{C^4(\overline{\Omega \cup \Omega_\delta})} \delta^2$. We therefore obtain the following truncation error estimate to the local limit:

Corollary 3.5. *Consider a kernel γ_δ satisfying the conditions in Lemma 3.1, a diffusion coefficient function $A(\cdot, \cdot)$ satisfying the conditions in (3.2), $u(\boldsymbol{x}) \in C^4(\overline{\Omega \cup \Omega_\delta})$, and fixed ratio $h/\delta < C_{pos}$. Quadrature weights obtained from (3.5) with the choice of $\boldsymbol{V}_{h,\boldsymbol{x}_i} = \boldsymbol{S}_{\gamma_\delta, \boldsymbol{x}}$ satisfy the following pointwise error estimate, with $C > 0$ independent of δ and h:*

$$\max_{\boldsymbol{x}_i \in \boldsymbol{V}_{h,\boldsymbol{x}_i}} \left| \mathcal{L}^0[u](\boldsymbol{x}_i) - \mathcal{L}_h^\delta[u](\boldsymbol{x}_i) \right| \leq C ||u||_{C^4(\overline{\Omega \cup \Omega_\delta})} \delta^2.$$

With the discrete maximum principle and the above truncation estimate results, we finally get the main results on the stability in maximum norm:

Lemma 3.6 (Stability). *Consider a bounded domain Ω and γ_δ satisfying the conditions in Lemma 3.1. Assume that $a(\cdot) \in C^\infty(\overline{\Omega})$, $A(\cdot, \cdot)$ satisfying the conditions in (3.2), and $\Omega \cup \Omega_\delta \in C^1$, then there exist generic constants C and $\delta_0 > 0$ such that when $\delta < \delta_0$ and $h < C_{pos}\delta$, solution to the discretized nonlocal diffusion problem (3.3) satisfies:*

$$\max_{\boldsymbol{x}_i \in \chi_h} |u_h^\delta(\boldsymbol{x}_i)| \leq \max_{\Omega_\delta} |u^D| + C \max_{\boldsymbol{x}_i \in \chi_h \cap \Omega} |f(\boldsymbol{x}_i)|.$$

Here C is independent of both h and δ.

Proof. We first construct a barrier function $\psi(\boldsymbol{x})$. With the properties of a, there exists a C^∞ solution $\hat{\psi}$ for the following classical diffusion problem [81]:

$$\mathcal{L}^0 \hat{\psi} = 2 \quad \text{on } \Omega \cup \Omega_\delta,$$

$$\hat{\psi} = 0 \quad \text{on } \partial(\Omega \cup \Omega_\delta),$$

where $\partial(\Omega \cup \Omega_\delta)$ denotes the exterior boundary of $\Omega \cup \Omega_\delta$. We then define $\psi(\boldsymbol{x}) := \hat{\psi}(\boldsymbol{x}) - \min_{\boldsymbol{z} \in \Omega \cup \Omega_\delta} \hat{\psi}(\boldsymbol{z})$, and notice that ψ satisfies: $\mathcal{L}^0 \psi = 2 > 0$, $0 \leq \psi \leq \left(\max_{\boldsymbol{z} \in \Omega \cup \Omega_\delta} \hat{\psi}(\boldsymbol{z}) - \min_{\boldsymbol{z} \in \Omega \cup \Omega_\delta} \hat{\psi}(\boldsymbol{z}) \right) := M_\psi$. Set $M_f := \max_{\boldsymbol{x}_i \in \chi_h \cap \Omega} |f(\boldsymbol{x}_i)|$. Since $\max_{\boldsymbol{x}_i \in \boldsymbol{V}_{h,\boldsymbol{x}_i}} \left| \mathcal{L}^0[\psi](\boldsymbol{x}_i) - \mathcal{L}_h^\delta[\psi](\boldsymbol{x}_i) \right| \leq C\delta^2$ as shown in Corollary 3.5, there exists a constant $\delta_0 > 0$ such that when $\delta < \delta_0$ we have $\mathcal{L}_h^\delta \psi \geq 1 > 0$. Then $\mathcal{L}_h^\delta(u_h^\delta + M_f \psi)(\boldsymbol{x}_i) = -f(\boldsymbol{x}_i) + M_f \geq 0$, and the discrete maximum principle yields

$$\max_{\boldsymbol{x}_i \in \chi_h} u_h^\delta(\boldsymbol{x}_i) \leq \max_{\boldsymbol{x}_i \in \chi_h} (u_h^\delta + M_f \psi)(\boldsymbol{x}_i) \leq \max_{\boldsymbol{x}_i \in \chi_h \cap \Omega_\delta} (u_h^\delta + M_f \psi)(\boldsymbol{x}_i)$$

$$\leq \max_{\Omega_\delta} |u^D| + M_f M_\psi = \max_{\Omega_\delta} |u^D| + M_\psi \max_{\boldsymbol{x}_i \in \chi_h \cap \Omega} |f(\boldsymbol{x}_i)|. \tag{3.10}$$

Similarly we can show that $\mathcal{L}_h^\delta(u_h^\delta - M_f \psi)(\boldsymbol{x}_i) = -f(\boldsymbol{x}_i) - M_f \leq 0$ and

$$\min_{\boldsymbol{x}_i \in \chi_h} u_h(\boldsymbol{x}_i) \geq -\max_{\Omega_\delta} |u^D| - M_\psi \max_{\boldsymbol{x}_i \in \chi_h \cap \Omega} |f(\boldsymbol{x}_i)|,$$

which together with (3.10) finishes the proof. $\qquad \square$

With the stability property of $\mathcal{L}_h^\delta$ and the truncation estimates in Lemmas 3.3-3.5 we proceed to prove the two types of convergence results in (3.1). We first consider the case with fixed δ and vanishing h. In particular, we investigate the convergence of numerical solution to nonlocal solution by combining Lemma 3.3 with the stability property:

Theorem 3.7 (Convergence to Deterministic Nonlocal Solution)**.** *Assume that the conditions in Lemma 3.3 and Lemma 3.6 are satisfied and $u^\delta \in C^1(\overline{\Omega \cup \Omega_\delta})$, then there exists a $\delta_0 > 0$ such that for a fixed δ satisfying $0 < \delta < \delta_0$ and $h < C_{pos}\delta$, the following convergence property holds for the numerical solution of* (3.3)*:*

$$||u_h^\delta - u^\delta||_{L^\infty(\chi_h)} \leq C(\delta) h^{\min(1,d-s)}, \tag{3.11}$$

where $C(\delta)$ is a generic constant independent of h but may depend on the (fixed) horizon size δ.

Proof. Apply the stability theorem to $u_h^\delta - u^\delta$, we immediately obtain

$$\max_{\boldsymbol{x}_i \in \chi_h} |u_h^\delta(\boldsymbol{x}_i) - u^\delta(\boldsymbol{x}_i)| \leq C \max_{\boldsymbol{x}_i \in \chi_h \cap \Omega} |\mathcal{L}_h^\delta u^\delta(\boldsymbol{x}_i) - \mathcal{L}^\delta u^\delta(\boldsymbol{x}_i)| \leq C(\delta) h^{\min(1,d-s)}.$$

$\qquad \square$

Next, we show the AC property of the meshfree method, when both δ and h vanish with a fixed ratio δ/h. In particular, we investigate the convergence rate of numerical solution to local limit by combining Lemma 3.4 and Corollary 3.5 with the stability property of $\mathcal{L}_h^\delta$:

Theorem 3.8 (Asymptotic Compatibility in Deterministic Nonlocal Problems)**.** *Assume that the conditions in Corollary 3.5 and Lemma 3.6 are satisfied, and $u^0 \in C^4(\overline{\Omega \cup \Omega_\delta})$, when applying the boundary condition*

23

$u^D(\boldsymbol{x}_i) = u^0(\boldsymbol{x}_i)$ for $\boldsymbol{x}_i \in \chi_h \cap \Omega_\delta$ then there exists a $\delta_0 > 0$ such that for any $0 < \delta < \delta_0$ and fixed ratio $h/\delta < C_{pos}$, the meshfree scheme (3.3) is asymptotically compatible, i.e.,

$$\left\|u_h^\delta - u^0\right\|_{L^\infty(\chi_h)} \le C\left\|u^0\right\|_{C^4(\overline{\Omega \cup \Omega_\delta})}\delta^2, \tag{3.12}$$

where C is a generic constant independent of δ and h.

Proof. Applying the stability theorem to $u_h^\delta - u^0$, we immediately obtain:

$$\max_{\boldsymbol{x}_i \in \chi_h} |u_h^\delta(\boldsymbol{x}_i) - u^0(\boldsymbol{x}_i)| \le C \max_{\boldsymbol{x}_i \in \chi_h \cap \Omega} |\mathcal{L}_h^\delta u^0(\boldsymbol{x}_i) - \mathcal{L}^0 u^0(\boldsymbol{x}_i)| \le C_2\left\|u^0\right\|_{C^4(\overline{\Omega \cup \Omega_\delta})}\delta^2$$

$\square$

Remark 3.9. In numerical tests of Sections 4-5, when verifying the AC convergence we generally set the boundary condition $u^D = u^0$ in Ω_δ. However, we note that it is generally not necessary to have u^0 defined in Ω_δ. When Ω is a Lipschitz domain, the above bounds can also be obtained for the general $u^0 \in C^4(\overline{\Omega})$, since one can extend u^0 to a C^4 function $\hat{u}^0$ in $\mathbb{R}^d$ (see, e.g., [82, Section 2]). Therefore, we can apply the derivation of Theorem 3.8 on $\hat{u}^0$ and apply the (nonlocal) boundary condition as $u^D = \hat{u}^0$. For further discussions on applying Dirichlet-type boundary conditions as an extended local solution, we refer interested readers to [72].

Remark 3.10. In numerical tests of Sections 4-5, we focus on the flat kernel with $s = 0$ for verification. In this case, from Theorems 3.7 and 3.8, we note that the optimal convergence rate to the nonlocal solution is $O(h)$ when $h \to 0$, while the optimal convergence to the local limit is $O(\delta^2)$ when $h, \delta \to 0$.

3.2. Stochastic: Probabilistic Collocation Method with Sparse Grids

To solve the stochastic problem introduced in Section 2.2, we employ the probabilistic collocation method (PCM) in the parametric space for its high resolution and ease of implementation by sampling at discrete points in random space [55, 83, 84]. Consider the stochastic equation (2.12), PCM can be seen as a Lagrange interpolation in the random space. In particular, let $\Theta_N = \{\boldsymbol{\xi}_k\}_{k=1}^K \subset \Gamma$ be a set of prescribed nodes such that the Lagrange interpolation in the random space Γ is poised in an interpolation space Γ_I, where N is the dimension of the parametric space. Then any function $v : \Gamma \to \mathbb{R}$ can be approximated using the Lagrange interpolation polynomial:

$$\mathcal{J}[v](\boldsymbol{\xi}) = \sum_{k=1}^K v(\boldsymbol{\xi}_k)J_k(\boldsymbol{\xi}),$$

where $J_k(\boldsymbol{\xi})$ is the Lagrange polynomial satisfying $J_k(\boldsymbol{\xi}) \in \Gamma_I$ and $J_k(\boldsymbol{\xi}_j) = \delta_{kj}$. Denoting $\hat{u}(\boldsymbol{x}, \boldsymbol{\xi}) := \sum_{k=1}^K u(\boldsymbol{x}, \boldsymbol{\xi}_k)J_k(\boldsymbol{\xi})$, the collocation procedure to solve the stochastic nonlocal equation is

$$R(\hat{u}(\boldsymbol{x}, \boldsymbol{\xi}))|_{\boldsymbol{\xi}_k} = 0, \quad \forall k = 1, \cdots, K,$$

24

where R is the residual of (2.12). With the property of Lagrange interpolation, we obtain

$$\begin{cases} -\mathcal{L}^{\delta}[u](\boldsymbol{x}, \boldsymbol{\xi}_k) = -\mathcal{D}[A(\boldsymbol{x}, \boldsymbol{y}, \boldsymbol{\xi}_k)\mathcal{G}[u(\boldsymbol{x}, \boldsymbol{\xi}_k)]] = f(\boldsymbol{x}) & \text{for } \boldsymbol{x} \in \Omega, \\ u(\boldsymbol{x}, \boldsymbol{\xi}_k) = u^D(\boldsymbol{x}), & \text{for } \boldsymbol{x} \in \Omega_{\delta}, \end{cases} \tag{3.13}$$

for $k = 1, \cdots, K$. Note that (3.13) is equivalent to solving K deterministic nonlocal diffusion problems, where the deterministic meshfree solver discussed in Section 3.1 can be readily applied. Therefore, the PCM approach can be implemented in an embarrassingly parallel way and the total computational cost is the product of the number of collocation points times the cost of the deterministic problem.

With the numerical solution of (3.13) on all collocation points $\boldsymbol{\xi}_i$, the statistical moments of the random solution can be evaluated:

$$\mathbb{E}[u](\boldsymbol{x}) \approx \mathbb{E}[\hat{u}](\boldsymbol{x}) = \int_{\Gamma} \sum_{k=1}^{K} u(\boldsymbol{x}, \boldsymbol{\xi}_k) J_k(\boldsymbol{\xi}) \rho(\boldsymbol{\xi}) d\boldsymbol{\xi},$$

$$\sigma[u](\boldsymbol{x}) \approx \sigma[\hat{u}](\boldsymbol{x}) = \sqrt{\int_{\Gamma} \left[\sum_{k=1}^{K} u(\boldsymbol{x}, \boldsymbol{\xi}_k) J_k(\boldsymbol{\xi}) \right]^2 \rho(\boldsymbol{\xi}) d\boldsymbol{\xi} - [\hat{u}](\boldsymbol{x})]^2},$$

and so on. Here ρ is the PDF of random variable $\boldsymbol{\xi}$. To further approximate the integral for above polynomials, we employ the quadrature rule approximation by choosing the set Θ_N as quadrature point set:

$$\mathbb{E}[u](\boldsymbol{x}) \approx \mathbb{E}[\hat{u}](\boldsymbol{x}) \approx \sum_{k=1}^{K} u(\boldsymbol{x}, \boldsymbol{\xi}_k)\mu_k, \tag{3.14}$$

$$\sigma[u](\boldsymbol{x}) \approx \sigma[\hat{u}](\boldsymbol{x}) \approx \sqrt{\sum_{k=1}^{K} u^2(\boldsymbol{x}, \boldsymbol{\xi}_k)\mu_k - [\mathbb{E}(\hat{u})(\boldsymbol{x})]^2}, \tag{3.15}$$

where $\{\mu_k\}_{k=1}^{K}$ is the set of corresponding quadrature weights.

There are mainly two different strategies for the selection of collocation point sets: the tensor products of 1D collocation point sets and sparse grid strategy for high dimensionality. In the tensor product strategy, one first construct a 1D interpolation for each dimension in the random space. For the i-th dimension, we take $\varpi_{(i)}$ numbers of nodal points $\Theta_1^{\varpi_{(i)}} = \{\xi_1^i, \cdots, \xi_{\varpi_{(i)}}^i\} \subset [-1, 1]$, a 1D interpolation for a smooth function v on the i-th dimension then writes:

$$\mathcal{U}^{\varpi_{(i)}}[v](\xi_{(i)}) = \sum_{k=1}^{\varpi_{(i)}} v(\xi_k^i) J_k^i(\xi_{(i)}) \tag{3.16}$$

where $J_k^i(\xi_{(i)})$ is the 1D Lagrange polynomial. Then for the multivariate case $v : \mathbb{R}^N \to \mathbb{R}$, the tensor

product formula is:

$$\mathcal{J}[v] = \left(\mathcal{U}^{\varpi(1)} \otimes \cdots \otimes \mathcal{U}^{\varpi(N)}\right)[v] = \sum_{k_1=1}^{\varpi(1)} \cdots \sum_{k_N=1}^{\varpi(N)} v\left(\xi_{k_1}^1, \cdots, \xi_{k_N}^N\right)\left(J_{k_1}^1 \otimes \cdots \otimes J_{k_N}^N\right). \qquad (3.17)$$

Notice here (3.17) requires $K = \Pi_{i=1}^N \varpi_{(i)}$ numbers of collocation points in total, which grows quickly when N gets large. Therefore, the tensor product strategy may be employed for problems with a small number of random dimensions, but its required number of collocation points K generally grows exponentially as N increases and makes the simulation non-feasible (see, e.g., [58]). Hence for problems with a relatively large random dimension, we employ the sparse grid strategy. In particular, we employ the sparse grid constructed by the Smolyak algorithm [85], which is a linear combination of tensor product formulas

$$\mathcal{J}[v] = \sum_{\zeta-N+1\le|\varpi|_{l_1}\le\zeta} (-1)^{\zeta-|\varpi|_{l_1}} \binom{N-1}{\zeta-|\varpi|_{l_1}} \left(\mathcal{U}^{\varpi(1)} \otimes \cdots \otimes \mathcal{U}^{\varpi(N)}\right) \qquad (3.18)$$

Here ζ is the sparseness parameter, $\varpi = (\varpi_{(1)}, \cdots, \varpi_{(N)}) \in \mathbb{N}^N$, $|\varpi|_{l_1} = \sum_{i=1}^N \varpi_{(i)}$, and $\varpi_{(i)}$ represents the number of collocation points in random dimension i. To compute (3.18), only evaluations on the sparse grids are needed:

$$\Theta_N = \bigcup_{\zeta-N+1\le|\varpi|_{l_1}\le\zeta} \left(\Theta_1^{\varpi(1)} \times \cdots \times \Theta_1^{\varpi(N)}\right). \qquad (3.19)$$

As shown in [86, 87], (3.18) is exact for $p(\xi) \in \mathbb{P}_{\zeta-N}(\mathbb{R}^N)$ (all polynomials of degree less than $\zeta - N$) and the total number of nodes $K \sim \frac{2N^{\zeta-N}}{(\zeta-N)!}$. Therefore, we may see that the sparse grid formulation typically requires a much smaller number of collocation points K than the full tensor product set and we will refer $\eta = \zeta - N$ as the "level" of the Smolyak formulation.

3.3. An Asymptotically Compatible Mesh-free PCM

Let δ be the horizon size, h be the grid size in space, and $K = K(\eta, N)$ be the total number of collocation points we use in the parameter space. We then denote the numerical solution to (2.12) by $u_{h,K}^\delta$. As $h \to 0$ and $K \to \infty$, we expect the numerical solution to converge to the exact solution u^δ for (2.12) in $L^2(\Omega) \otimes L_\rho^2(\Gamma)$. In addition, our numerical method is asymptotically compatible, i.e., $u_{h,K}^\delta \to u^0$ as $h \to 0$, $K \to \infty$, and $\delta \to 0$, where u^0 is the exact solution for (2.15). The error estimate can be facilitated by introducing intermediate functions u_K^δ and u_K^0, the semi-discrete solutions to (2.12) and (2.15) respectively. Then we split the errors into

$$\begin{cases} u^\delta - u_{h,K}^\delta = (u^\delta - u_K^\delta) + (u_K^\delta - u_{h,K}^\delta) \\ u^0 - u_{h,K}^\delta = (u^0 - u_K^0) + (u_K^0 - u_{h,K}^\delta). \end{cases}$$

For each $\xi \in \Gamma$,

$$u_K^\delta(\xi) = \sum_{k=1}^K u^\delta(\xi_k) J_k(\xi), \text{ and } u_{h,K}^\delta(\xi) = \sum_{k=1}^K u_h^\delta(\xi_k) J_k(\xi).$$

26

The estimates of $\|u^\delta(\boldsymbol{\xi}_k) - u_h^\delta(\boldsymbol{\xi}_k)\|_{L^2(\Omega)}$ for each $\boldsymbol{\xi}_k$ are followed by the estimates in Section 3. So we have $\|u_K^\delta(\boldsymbol{\xi}) - u_{h,K}^\delta(\boldsymbol{\xi})\|_{L^2(\Omega)} \to 0$ for each $\boldsymbol{\xi} \in \Gamma$ and therefore $\|u_K^\delta - u_{h,K}^\delta\|_{L^2(\Omega)\otimes L^2_\rho(\Gamma)} \to 0$ as $h \to 0$. The rate at which $\|u_K^\delta - u_{h,K}^\delta\|_{L^2(\Omega)\otimes L^2_\rho(\Gamma)}$ converges to zero follows the estimates in Section 3. Moreover, we have $\|u^0(\boldsymbol{\xi}) - u^\delta(\boldsymbol{\xi})\|_{L^2(\Omega)} \le C\delta^2$ for any $\boldsymbol{\xi}$ as long as $u^0 \in C^4(\overline{\Omega \cup \Omega_\delta})$. Therefore we only need to estimate $u^\delta - u_K^\delta$.

From the analytic regularity, $\boldsymbol{\xi} \mapsto u^\delta(\boldsymbol{\xi})$ is a $S_\delta(\Omega)$-valued map that admits an analytic extension to an open neighborhood $\mathcal{A} \subset \mathbb{C}^N$ of Γ. Moreover, we know that $\max_{\hat{\boldsymbol{\xi}}\in\mathcal{A}}\|u^\delta(\hat{\boldsymbol{\xi}})\|_{S_\delta(\Omega)}$ is uniformly bounded and independent of δ. Therefore, the estimate of $u^\delta - u_K^\delta$ is followed exactly from [55]. Here we present the following result, whose proof can be found in [55, Theorems 3.10-3.11]. From now on we use L^∞ estimate in the parametric space Γ, and the $L^2_\rho(\Gamma)$ norm is bounded by the $L^\infty(\Gamma)$ norm.

Lemma 3.11. *There exists $C_1 > 0$ and $\beta_1 > 0$ depending on N and the analytic region $\mathcal{A}$ such that*

$$\max_{\boldsymbol{\xi}\in\Gamma} \|u^\delta(\boldsymbol{\xi}) - u_K^\delta(\boldsymbol{\xi})\|_{S_\delta(\Omega)} \le C_1 K^{-\beta_1}. \tag{3.20}$$

Moreover, when $\eta > \frac{N}{\log(2)}$, there exists $C_2 > 0$, $C_3 > 0$ and $\beta_2 > 0$ depending on N and the analytic region $\mathcal{A}$, and $\beta_3 > 0$ depending only on N such that

$$\max_{\boldsymbol{\xi}\in\Gamma} \|u^\delta(\boldsymbol{\xi}) - u_K^\delta(\boldsymbol{\xi})\|_{S_\delta(\Omega)} \le C_2 K^{\beta_2} e^{-C_3 K^{\beta_3}}. \tag{3.21}$$

Equation (3.20) shows at least algebraic convergence with respect to the number of collocation points K, while equation (3.21) shows the subexponential convergence when the level of Smolyak formulation $\eta > \frac{N}{\log(2)}$. In the numerical experiments below, we will choose large enough η so as to observe the subexponential convergence. Based on Lemma 3.11 and the above discussions, we have the following convergence theorems.

Theorem 3.12. *Assume that $\max_{\boldsymbol{\xi}\in\Gamma}\|u^\delta(\boldsymbol{\xi})\|_{C^1(\overline{\Omega\cup\Omega_\delta})} < \infty$, then there exists a $\delta_0 > 0$ such that for a fixed δ satisfying $0 < \delta < \delta_0$ and any $h < C_{pos}\delta$, we have*

$$\|u^\delta - u_{h,K}^\delta\|_{L^2(\Omega)\otimes L^\infty(\Gamma)} \le C(\delta)\Lambda(\eta,N)h^{\min(1,d-s)} + C_1 K^{-\beta_1}.$$

Moreover, when $\eta > \frac{N}{\log(2)}$, we have

$$\|u^\delta - u_{h,K}^\delta\|_{L^2(\Omega)\otimes L^\infty(\Gamma)} \le C(\delta)\Lambda(\eta,N)h^{\min(1,d-s)} + C_2 K^{\beta_2} e^{-C_3 K^{\beta_3}}.$$

The constants C_1, C_2, C_3, β_1, β_2, β_3 are defined in Lemma 3.11, $C(\delta)$ is defined in Theorem 3.7, and $\Lambda(\eta, N)$ is the Lebesgue constant associated with the sparse grid interpolation, satisfying

$$\Lambda(\eta,N) \le \sum_{\zeta-N+1\le|\boldsymbol{\varpi}|_{l_1}\le\zeta} \binom{N-1}{\zeta-|\boldsymbol{\varpi}|_{l_1}} \prod_{j=1}^{N} \left(\frac{2}{\pi}\log(\varpi_{(j)}+1)+1\right). \tag{3.22}$$

27

Proof. Let $u^\delta - u^\delta_{h,K} = (u^\delta - u^\delta_K) + (u^\delta_K - u^\delta_{h,K})$. Notice that $\Lambda(\eta, N)$ is the Lebesgue constant associated with the sparse grid interpolation, i.e.,

$$\Lambda(\eta, N) := \sup_{v \in C(\Gamma)} \frac{\|\mathcal{J}[v]\|_{L^\infty}}{\|v\|_{L^\infty}},$$

where $\mathcal{J}[v]$ is given by (3.18). Then by Theorem 3.7, we have

$$\|u^\delta_K - u^\delta_{h,K}\|_{L^2(\Omega)\otimes L^\infty(\Gamma)} \le \Lambda(\eta, N)\|u^\delta - u^\delta_h\|_{L^2(\Omega)\otimes L^\infty(\Gamma)} \le \Lambda(\eta, N)C(\delta)h^{\min(1,d-s)}.$$

Now for each $\boldsymbol{\varpi} = (\varpi_{(1)}, \cdots, \varpi_{(N)}) \in \mathbb{N}^N$, the Lebesgue constant of the interpolation operator $\mathcal{U}^{\varpi_{(1)}} \otimes \cdots \otimes \mathcal{U}^{\varpi_{(N)}}$ is given by $\prod_{j=1}^N L(\varpi_{(j)})$, where $L(m)$ is the classical Lebesgue constant for Clenshaw–Curtis abscissas in 1D, which is estimated by (see, e.g., [88])

$$L(m) \le \frac{2}{\pi}\log(m+1) + 1.$$

Therefore by the definition of $\mathcal{J}[v]$ in (3.18), we have the estimate of $\Lambda(\eta, N)$ in (3.22). and The theorem is then a combination of the above estimates and Lemma 3.11. □

Theorem 3.13. *Let δ_0 be the constant defined in Lemma. Assume that $\max_{\boldsymbol{\xi}\in\Gamma}\|u^0(\boldsymbol{\xi})\|_{C^4(\overline{\Omega\cup\Omega_\delta})} < \infty$. Then for any δ with $0 < \delta < \delta_0$ and fixed ratio $h/\delta < C_{pos}$, we have*

$$\|u^0 - u^\delta_{h,K}\|_{L^2(\Omega)\otimes L^\infty(\Gamma)} \le C\Lambda(\eta, N)\delta^2 + C_1 K^{-\beta_1}.$$

Moreover, if $\eta > \frac{N}{\log(2)}$, we have

$$\|u^0 - u^\delta_{h,K}\|_{L^2(\Omega)\otimes L^\infty(\Gamma)} \le C\Lambda(\eta, N)\delta^2 + C_2 K^{\beta_2}e^{-C_3 K^{\beta_3}}.$$

The constants C_1, C_2, C_3, β_1, β_2, β_3 are defined in Lemma 3.11, and $\Lambda(\eta, N)$ is estimated by (3.22). The constant C, which depends on $\max_{\boldsymbol{\xi}\in\Gamma}\|u^0(\boldsymbol{\xi})\|_{C^4(\overline{\Omega\cup\Omega_\delta})}$, is independent of the parameters δ, h, η and N.

Proof. Let $u^0 - u^\delta_{h,K} = (u^0 - u^0_K) + (u^0_K - u^\delta_{h,K})$. For each $\boldsymbol{\xi} \in \Gamma$, we can apply Theorem 3.8 to get $\|u^0(\boldsymbol{\xi}) - u^\delta_h(\boldsymbol{\xi})\|_{L^2(\Omega)} \le C\delta^2$, where C depends on $\|u^0(\boldsymbol{\xi})\|_{C^4(\overline{\Omega\cup\Omega_\delta})}$. Therefore, we have

$$\|u^0_K - u^\delta_{h,K}\|_{L^2(\Omega)\otimes L^\infty(\Gamma)} \le \Lambda(\eta, N)\|u^0 - u^\delta_h\|_{L^2(\Omega)\otimes L^\infty(\Gamma)} \le C\Lambda(\eta, N)\delta^2.$$

Then the theorem is combination of above estimate and Lemma 3.11 when applied to $\delta = 0$. □

Remark 3.14. Notice that in the proof of numerical convergence for the meshfree method, we made relatively strong regularity assumptions that the nonlocal solution $\boldsymbol{u}^\delta \in C^1(\overline{\Omega\cup\Omega_\delta})$ and the local solution $\boldsymbol{u}^0 \in C^4(\overline{\Omega\cup\Omega_\delta})$. However, in many real-world applications regarding both local and nonlocal cases, this

could not be guaranteed. Therefore, in the numerical tests of Sections 4-5, besides testing the numerical convergences for manufactured solutions satisfying $\boldsymbol{u}^\delta \in C^1(\overline{\Omega \cup \Omega_\delta})$ in the first two tests and $\boldsymbol{u}^0 \in C^4(\overline{\Omega \cup \Omega_\delta})$ in the third and fourth cases, we also investigate the convergence of numerical nonlocal solutions to its local limit when $\boldsymbol{u}^0 \notin C^4(\overline{\Omega \cup \Omega_\delta})$, in the last two numerical tests. We notice that the later is not covered by Theorem 3.13 and therefore we have no theoretical guarantee on the numerical convergence. So these two tests provides empirical studies on the applicability of our proposed algorithm when the regularity requirements are not satisfied.

4. Numerical Verification of Convergences

In this section, we numerically verify the proposed approach by investigating the two types of convergences: the consistency to nonlocal solutions and then the asymptotic compatibility to local companions[4]. In particular, we study the L^2 errors for the first two statistical moments, the mean and standard deviation (std). Let $u_{h,K}^\delta$ represent the numerical solution with spatial grid size h in meshfree methods and K samples in sparse grid PCM, u^δ represents the analytical nonlocal solution and u^0 stands for the analytical local limit, in Section 4.1 we investigate the convergence of numerical solutions to the nonlocal analytical solution with vanishing h and increasing sample numbers K by calculating:

$$\|\mathbb{E}(u_{h,K}^\delta) - \mathbb{E}(u^\delta)\|_{L_2(\Omega)} \quad \text{and} \quad \|\sigma(u_{h,K}^\delta) - \sigma(u^\delta)\|_{L_2(\Omega)}, \tag{4.1}$$

where the mean and standard deviation of $u_{h,K}^\delta$ are numerically evaluated with the quadrature rule approximation in (3.14)-(3.15). Similarly, in Section 4.2 we investigate the convergence of numerical solutions to the local limit as K increases and δ, h goes to 0 simultaneously under the δ-convergence limit. In particular we calculate:

$$\|\mathbb{E}(u_{h,K}^\delta) - \mathbb{E}(u^0)\|_{L_2(\Omega)}, \quad \text{and} \quad \|\sigma(u_{h,K}^\delta) - \sigma(u^0)\|_{L_2(\Omega)}. \tag{4.2}$$

In all numerical tests, we consider 1D and 2D nonlocal diffusion problems with flat kernels ($s = 0$). In particular, for 1D problems we set $\gamma_\delta(|\boldsymbol{x} - \boldsymbol{y}|) := \frac{3}{2\delta^3}$ and for 2D problems $\gamma_\delta(|\boldsymbol{x} - \boldsymbol{y}|) := \frac{4}{\pi\delta^4}$.

4.1. Consistency with the Stochastic Nonlocal Solution

In this section we study the consistency of the numerical solution to the nonlocal analytical solution, on both 1D and 2D physical domains.
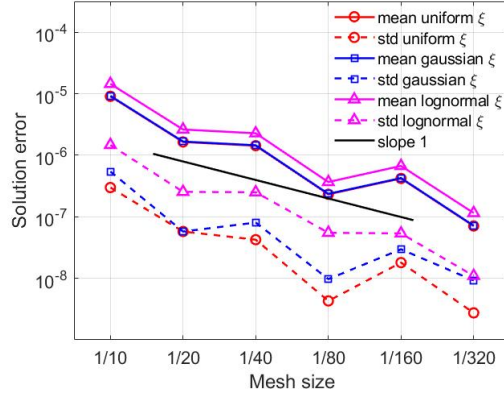
(a) Convergence with refinement in the physical space.
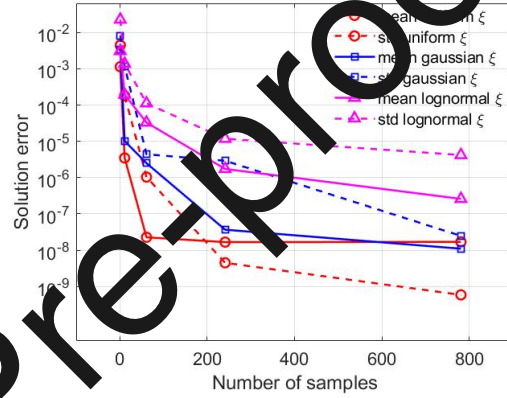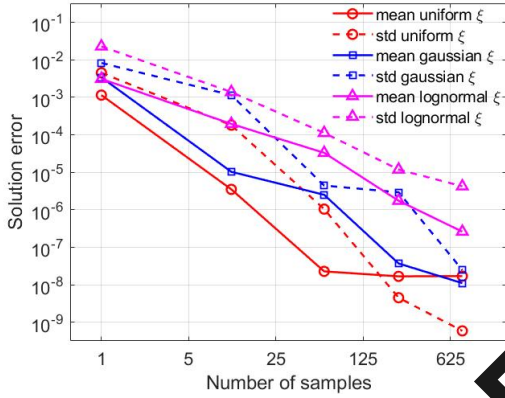
(b) Convergence with sample numbers in the log scale.   (c) Convergence with sample numbers in the linear scale.

Figure 1: Test 1: consistency study of the numerical solution to the nonlocal analytical solution on a problem with 1D physical domain and 5D parametric space. Results in (a) are generated with 781 samples, which corresponds to Smolyak formulation level 5. The data points in (b) and (c) correspond to Smolyak formulation levels $\eta = 1, \cdots, 5$.

*Test 1: consistency study on a problem with 1D physical domain and 5D parametric space*

We consider a case with 1D physical domain $\Omega = [-1, 1]$ and 5D parametric space $\boldsymbol{\xi} = (\xi_{(1)}, \cdots, \xi_{(5)})$, where $\xi_{(i)}$ are i.i.d. random variables. We manufacture the nonlocal analytical solution

$$u^{\delta}(x, \boldsymbol{\xi}) = \cos(0.5x)/(5 + \cos(\xi_{(1)}) + \sin(2\xi_{(2)}) + \cos(3\xi_{(3)}) + \sin(4\xi_{(4)}) + \cos(5\xi_{(5)})),$$

with fixed $\delta = 0.38$, nonlocal diffusion coefficient

$$A(x, y, \boldsymbol{\xi}) = (2 + \cos(0.5(x + y)))(5 + \cos(\xi_{(1)}) + \sin(2\xi_{(2)}) + \cos(3\xi_{(3)}) + \sin(4\xi_{(4)}) + \cos(5\xi_{(5)})),$$

---

[4]Notice that although we assumed $\Gamma = \prod_{i=1}^{N}[-1, 1] \subset \mathbb{R}^N$ in Sections 2-3, in numerical tests we investigate and numerically verify our analysis on more general cases.

and loading

$$f(x) = -\frac{3}{\delta^3}\Big(\frac{1}{2}\big(-2\sin(0.5(3x+\delta)) + \sin(0.5(3x+2\delta)) - 3\delta\cos(0.5x) + 6\sin(0.5(x+\delta))\big)$$
$$-\frac{1}{2}\big(-2\sin(0.5(3x-\delta)) + \sin(0.5(3x-2\delta)) + 3\delta\cos(0.5x) + 6\sin(0.5(x-\delta))\big)\Big).$$

In $\Omega_\delta := [-1-\delta, -1) \cup (1, 1+\delta]$, Dirichlet-type boundary conditions are applied:

$$u^D(x,\boldsymbol{\xi}) := \cos(0.5x)/(5 + \cos(\xi_{(1)}) + \sin(2\xi_{(2)}) + \cos(3\xi_{(3)}) + \sin(4\xi_{(4)}) + \cos(5\xi_{(5)})).$$

Three types of distributions are considered for $\xi_{(i)}$, $i = 1, \cdots, 5$: the uniform distribution $\xi_{(i)}^{(1)} \sim \mathcal{U}[-0.1, 0.1]$, the Gaussian distribution $\xi_{(i)}^{(2)} \sim \mathcal{N}(0, 0.1^2)$ and the lognormal distribution $\xi_{(i)}^{(3)} = \exp(\xi_{(i)}^{(2)})$.

Numerical results are provided in Figure 1. With fixed Smolyak sparse grid level $\eta = 5$, we demonstrate the spatial convergence of numerical solution for grid sizes $h = \{1/10, 1/20, 1/40, 1/80, 1/160, 1/320\}$ in Figure 1(a). First-order convergence $O(h)$ is observed. In Figures 1(b) and 1(c), we employ a fixed grid size $h = 1/1280$ and demonstrate the convergence of solution error with increasing sparse grid level $\eta = 1, \cdots, 5$ in the parametric space. When $\eta \geq 3$, the numerical error of mean for uniform distribution reaches a convergence plateau because of the spatial discretization error. Noting that we have $\eta < N/\log(2) \approx 7.5$ in this case, algebraic convergence of the sparse grid PCM is verified for all three types of distributions. Therefore, the $O(h)$ spatial convergence and the algebraic convergence of the sparse grid PCM together verify the estimates in Theorem 3.12.

Test 2: consistency study on a problem with 2D physical domain and 1D parametric space

We now consider a case on a square physical domain $\Omega = [0, 1] \times [0, 1]$ depending on a random variable ξ. With fixed $\delta = 0.525$ and nonlocal diffusion coefficient $A(\boldsymbol{x}, \boldsymbol{y}, \xi) = (2+\xi)[2+\cos(A(x_{(1)}+y_{(1)}))\cos(B(x_{(2)}+y_{(2)}))]/\delta^4$, we consider the manufactured nonlocal analytical solution

$$u^\delta(\boldsymbol{x}, \xi) = u(x_{(1)}, x_{(2)}, \xi) = \cos(Ax_{(1)})\sin(Bx_{(2)})/(2+\xi).$$

Here we take $A = B = 2\pi$ in this example. For $\boldsymbol{x} \in \Omega_\delta$, Dirichlet-type boundary conditions are applied as: $u^D(\boldsymbol{x}, \xi) := \cos(Ax_{(1)})\sin(Bx_{(2)})/(2+\xi)$. Four types of popular distributions are studied: the uniform distribution $\xi^{(1)} \sim \mathcal{U}[-0.1, 0.1]$, the Gaussian distribution $\xi^{(2)} \sim \mathcal{N}(0, 0.1^2)$, the lognormal distribution $\xi^{(3)} = \exp(\xi^{(2)})$, and the rescaled Weibull distribution $\xi^{(4)} = 0.5\hat{\xi}$. Here $\hat{\xi}$ is the Weibull random variable with the shape parameter $k = 5.0$ and the scale parameter $\lambda = 1$.

Numerical convergence to the nonlocal analytical solution is demonstrated in Figure 2. With 5 collocation points in PCM, we investigate the spatial convergence of numerical solution for grid sizes $h = \{1/4, 1/8, 1/16, 1/32, 1/64\}$ in Figure 2(a). An $O(h)$ convergence rate is observed. In Figures 2(b) and 2(c) we consider a fixed grid size $1/32$ and study the convergence of solution error with increasing sample num-
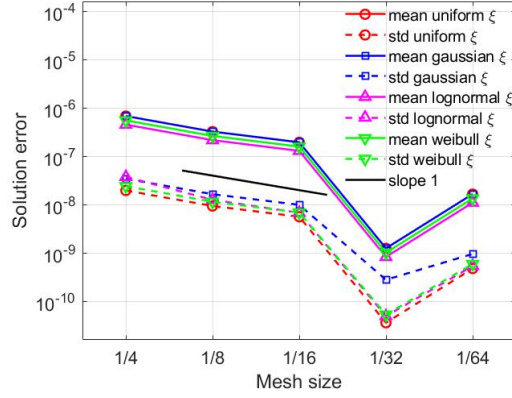
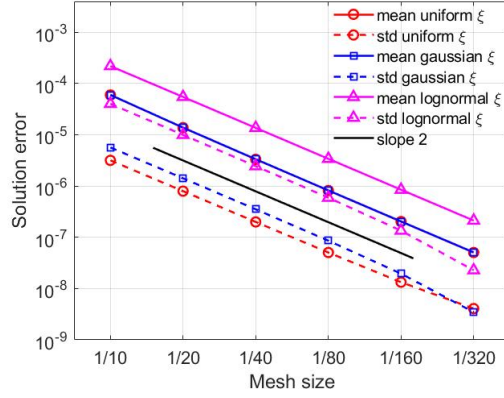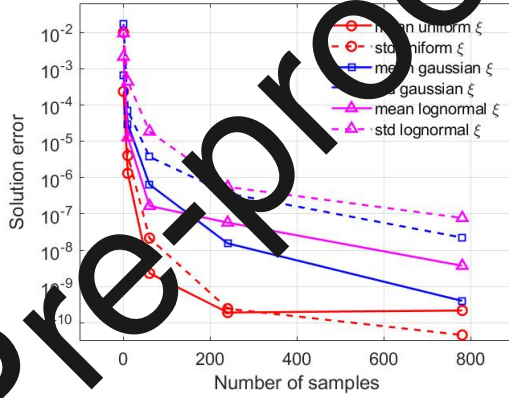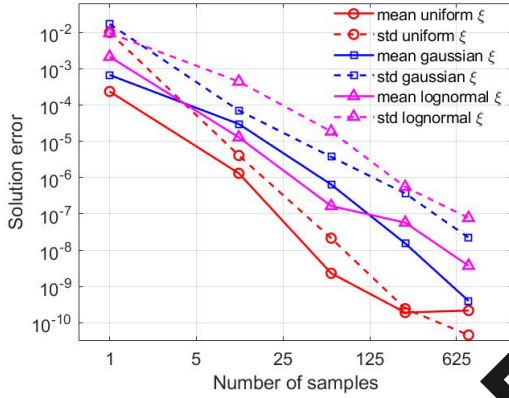(a) Convergence with refinement in the physical space.
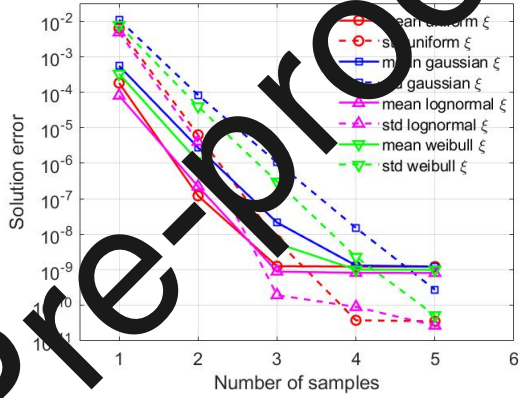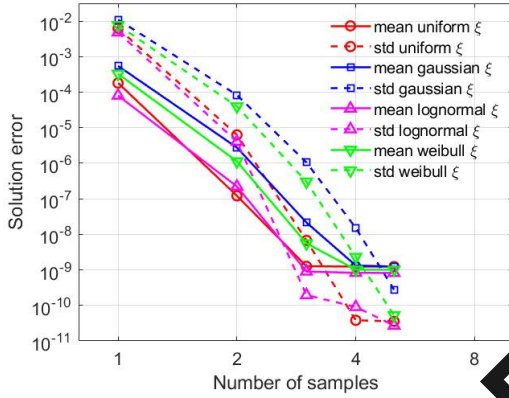
(b) Convergence with sample numbers in the log scale.   (c) Convergence with sample numbers in the linear scale.

Figure 2: Test 2: consistency study of the numerical solution to the nonlocal analytical solution on a problem with 2D physical domain and 1D parametric space. Results in (a) are generated with 5 samples, which corresponds to Smolyak formulation level 5. The data points in (b) and (c) correspond to Smolyak formulation levels $\eta = 1, \cdots, 5$.

bers in PCM. In particular, we take coarse grid levels $\eta \in \{1, \cdots, 5\}$. When $\eta \geq 4$, the numerical errors of mean for all distribution types reach a convergence plateau because of the spatial discretization error. When $\eta > N/\log(2) \approx 1.5$, sub-exponential convergence is observed for all four types of considered distributions before reaching this plateau, which again verifies Theorem 3.12.

4.2. Asymptotic Compatibility (AC) to the Stochastic Local Limit

In this section we investigate the asymptotic compatibility (AC) of the proposed approach by studying the convergence of its numerical solution to the corresponding local limit when $\delta, h \to 0$. In particular, we focus on the δ-convergence limit and fix the ratio between δ and h. Following the conventions in [37, 89, 90], in all tests we consider the nonlocal diffusion coefficient as the harmonic mean of the local diffusion coefficient: $A(\boldsymbol{x}, \boldsymbol{y}, \boldsymbol{\xi}) = 2/(a^{-1}(\boldsymbol{x}, \boldsymbol{\xi}) + a^{-1}(\boldsymbol{y}, \boldsymbol{\xi}))$.

32

(a) Convergence with $\delta, h \to 0$ in the physical space.

(b) Convergence with sample numbers in the log scale. (c) Convergence with sample numbers in the linear scale.
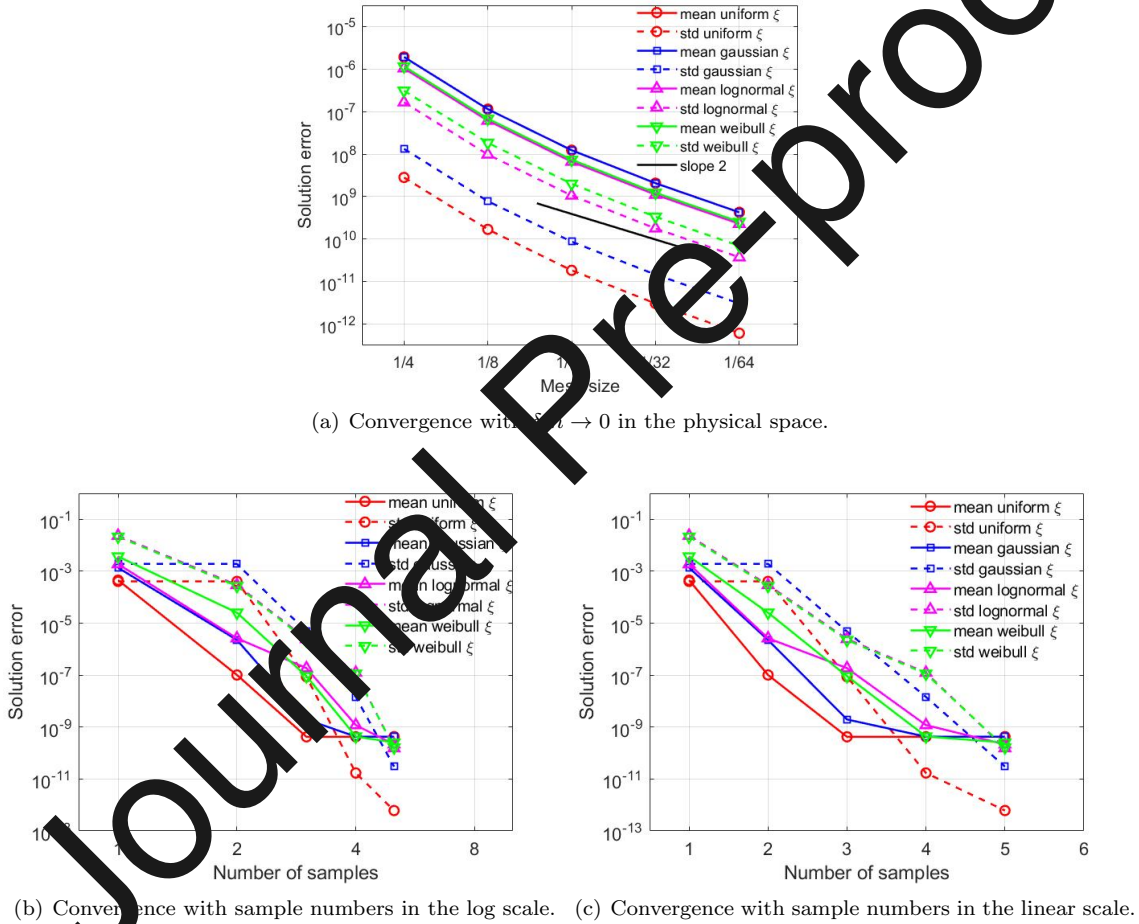
Figure 3: Test 1: asymptotic compatibility study of the numerical solution to the analytical local limit on a problem with 1D physical domain and 5D parametric space. Results in (a) are generated with 781 samples, which corresponds to Smolyak formulation level 5. The data points in (b) and (c) corresponds to Smolyak formulation levels $\eta = 1, \cdots, 5$.

Test 1: AC study on a problem with 1D physical domain and 5D parametric space

We consider a case with 1D physical domain $\Omega = [-1, 1]$ and 5D parametric space $\boldsymbol{\xi} = (\xi_{(1)}, \cdots, \xi_{(5)})$, where $\xi_{(i)}$ are i.i.d. random variables. The analytical local solution is given by

$$u^0(x, \boldsymbol{\xi}) = \frac{\log(12 + (1 + \exp(\sin(\xi_{(1)})) + \cos(\xi_{(2)}) + \exp(\sin(\xi_{(3)})) + \cos(\xi_{(4)}) + \exp(\sin(2\xi_{(5)}))) \sin(x))}{+ \exp(\sin(\xi_{(1)})) + \cos(\xi_{(2)}) + \exp(\sin(\xi_{(3)})) + \cos(\xi_{(4)}) + \exp(\sin(2\xi_{(5)})))},$$

with fixed loading $f(x) = \sin(x)$ and local diffusion coefficient

$$a(x, \boldsymbol{\xi}) = 12 + (1 + \exp(\sin(\xi_{(1)})) + \cos(\xi_{(2)}) + \exp(\sin(\xi_{(3)})) + \cos(\xi_{(4)}) + \exp(\sin(2\xi_{(5)}))) \sin(x).$$

For $x \in \Omega_\delta := [-1 - \delta, -1) \cup (1, 1 + \delta]$, Dirichlet-type boundary conditions are applied as: $u^D(x, \boldsymbol{\xi}) := u^0(x, \boldsymbol{\xi})$. Three types of distributions are considered for $\xi_{(i)}$, $i = 1, \cdots, 5$: the uniform distribution $\xi_{(i)}^{(1)} \sim \mathcal{U}[-0.1, 0.1]$, the Gaussian distribution $\xi_{(i)}^{(2)} \sim \mathcal{N}(0, 0.1^2)$ and the lognormal distribution $\xi_{(i)}^{(3)} = \exp(\xi_{(i)}^{(2)})$.

33

Numerical results are provided in Figure 3. With fixed ratio $\delta/h = 3.8$ and Smolyak sparse grid level $\eta = 5$, in Figure 3(a) we show the error of numerical solution with respect to the analytical local limit for grid sizes $h = \{1/10, 1/20, 1/40, 1/80, 1/160, 1/320\}$. Second-order convergence $O(\delta^2)$ is observed. The proposed approach is therefore AC and the observed convergence rate is consistent with our AC analysis in Theorem 3.13. In Figures 3(b) and 3(c) we fix $h = 1/5000$ and $\delta = 3.8h$, and show the convergence of solution error with increasing sparse grid level $\eta = 1, \cdots, 5$ in the parametric space. Noting that we have $\eta < N/\log(2) \approx 7.5$ in this case, algebraic convergence of the sparse grid PCM is verified for all types of distributions, which is also consistent with the analysis in Theorem 3.13.

Test 2: AC study on a problem with 2D circular domain and 1D parametric space

(a) Convergence with $\delta, h \to 0$ in the physical space.

(b) Convergence with sample numbers in the log scale. (c) Convergence with sample numbers in the linear scale.
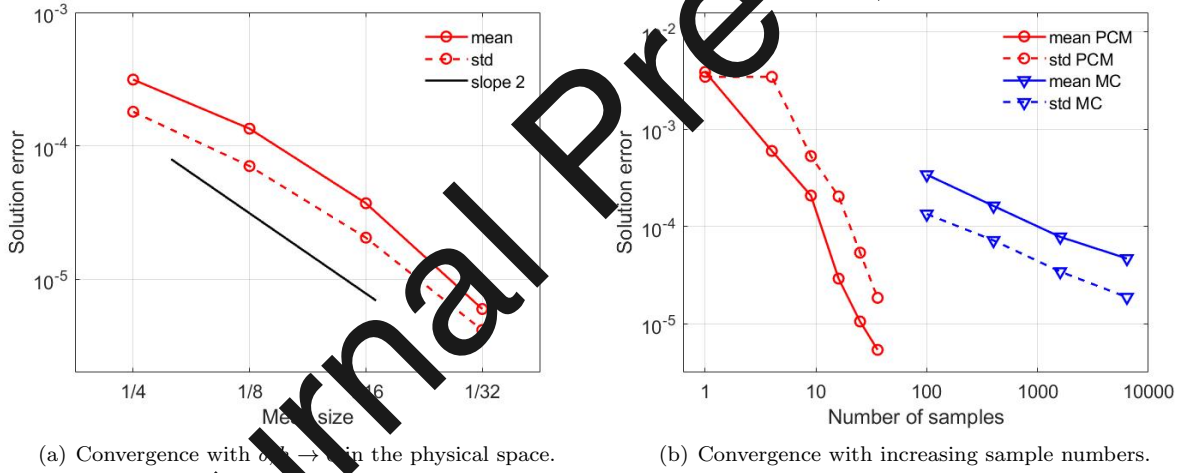
Figure 4: Test 2: asymptotic compatibility study of the numerical solution to the analytical local limit on a problem with 2D circular domain and 1D parametric space. Results in (a) are generated with 7 samples, which corresponds to Smolyak formulation level 5. The data points in (b) and (c) correspond to Smolyak formulation levels $\eta = 1, \cdots, 5$.

We next consider a more general physical domain with a curvilinear boundary. In particular, we employ a circular physical domain $\Omega = B_1(0)$ and consider 1D parametric space. Under radical coordinate and with local diffusion coefficient $a(r, \theta, \xi) = 1/(2 + \cos(\xi)\sin(r^2))$, loading $f(r, \theta) = 1$, the classical diffusion problem

yields the analytical local solution

$$u^0(r, \theta, \xi) = \frac{1}{4}(2r^2 - \cos(\xi)\cos(r^2)).$$

In Ω_δ, Dirichlet-type boundary conditions are applied as: $u^D(r, \theta, \xi) := u^0(r, \theta, \xi)$. Four types of distributions are considered in this case: the uniform distribution $\xi^{(1)} \sim \mathcal{U}[-0.1, 0.1]$, the Gaussian distribution $\xi^{(2)} \sim \mathcal{N}(0, 0.1^2)$, the lognormal distribution $\xi^{(3)} = \exp(\xi^{(2)})$, and the Weibull distribution $\xi^{(4)}$ with the shape parameter $k = 5.0$ and the scale parameter $\lambda = 1$.

Numerical results are shown in Figure 4. In Figure 4(a) we consider fixed $\delta/h = 3.8$ and 7 samples with sparse grid PCM, then study the convergence of numerical solution to the analytical local limit with decreasing grid size from $h = 1/4$ to $1/64$. An $O(\delta^2)$ is obtained. In Figures 4(b) and 4(c) we employ a fixed grid size $h = 1/64$ and $\delta = 3.8h$, then demonstrate the convergence rate of PCM with increasing number of samples corresponding to $\eta = 1, \cdots, 5$. Before the numerical error reaches a convergence plateau due to the spatial discretization error, an sub-exponential convergence is obtained with increasing sample numbers.

Test 3: AC study on a problem with 2D square domain and 2D parametric space

(a) Convergence with $\delta, h \to 0$ in the physical space.   (b) Convergence with increasing sample numbers.

Figure 5: Test 3: asymptotic compatibility study of the numerical solution to the analytical local limit on a problem with 2D square domain and 2D parametric space. Results in (a) are generated with 100 samples. The data points in (b) correspond to Smolyak formulation level $\eta = 1, \cdots, 6$.

We now consider a 2D square domain $\Omega = [-1, 1] \times [-1, 1]$ and 2D parametric space $\boldsymbol{\xi} = (\xi_{(1)}, \xi_{(2)})$, $\xi_{(i)} \sim \mathcal{U}[-0.1, 0.1]$, with loading $f(\boldsymbol{x}) = 1$ and local diffusion coefficient

$$a(\boldsymbol{x}, \boldsymbol{\xi}) = 3 + \sum_{k=1}^{2} \frac{\cos(30\xi_{(k)}) - 1}{k^2} \cos(2kx_{(1)}) \sin(2kx_{(2)}).$$

Since there is no analytical expression for the local limit, $u^0(\boldsymbol{x}, \boldsymbol{\xi})$ is generated numerically based on a spectral method solver on Ω. In this example, we adopt the "interior boundary layer" setting for its simplicity. To

35

provide a nonlocal Dirichlet-type boundary condition, we set $u^D(\boldsymbol{x}, \boldsymbol{\xi}) := u^0(\boldsymbol{x}, \boldsymbol{\xi})$ and apply this boundary condition on $\Omega_{-\delta}$.

Numerical results are provided in Figure 5. With 100 collocation points in PCM and fixed $\delta/h = 2.8$, we investigate the spatial convergence of numerical solution with decreasing grid size from $h = 1/4$ to $1/32$ in Figure 5(a). Second order convergence is observed, which is consistent with our analysis. In Figure 5(b) we employ fixed grid size $h = 1/32$, $\delta = 2.8h$ and show the convergence of numerical solutions obtained from MC simulations and the PCM results with respect to the increase of sample points. Here the sparse grid levels are taken as $\eta = 1, \cdots, 6$. When $\eta > N/\log(2) \approx 3$, sub-exponential convergence is observed for PCM, and the results also indicate that PCM can achieve a similar accuracy with much smaller number of sample points than MC. Although the regularity requirement of $\boldsymbol{u}^0$ in Theorem 3.13 is generally not guaranteed in this test, an algebraic convergence to the local limit $\boldsymbol{u}^0$ is still observed empirically for the numerical nonlocal solution.

Remark 4.1. By the classical elliptic regularity theory for convex polygonal domains, one can show that $u^0(\boldsymbol{\xi}) \in H^2(\Omega)$ for $\boldsymbol{\xi} \in \Gamma$. Although Theorem 3.13 requires u^0 to be in a stronger space $C^4(\overline{\Omega \cup \Omega_\delta})$, we do observe second order convergence in δ with our numerical method. The C^4 assumption agrees with classical numerical analysis results for strong form discretization of elliptic problems. How to improve the regularity assumption in Theorem 3.13 remains an open question.

5. Stochastic Nonlocal Diffusion Problem in Randomly Heterogeneous Domain

5.1. Stochastic Representation and Karhunen-Loève Expansion

We use the Karhunen-Loève (K-L) expansion to represent the random field $a(\boldsymbol{x}, \omega)$. In general, consider a square-integrable stochastic random field $F(\boldsymbol{x}, \omega)$ defined on $\Omega \times \Omega_p$, where Ω is a subset of $\mathbb{R}^d$ (d is the dimension) and Ω_p is the sample space of a probability space $(\Omega_p, \mathcal{F}, \mathcal{P})$. If $F(\boldsymbol{x}, \omega)$ has a constant mean and a continuous covariance function (also called kernel function) $\Xi(\boldsymbol{x}, \boldsymbol{y})$, then $F(\boldsymbol{x}, \omega)$ can be represented by the following Karhunen-Loève (KL) expansion:

$$F(\boldsymbol{x}, \omega) = F_0 + \sum_{n=1}^{\infty} \sqrt{\lambda_i} \phi_i(\boldsymbol{x}) \xi_{(i)}(\omega),$$

where F_0 is the constant mean, (λ_i, ϕ_i) are eigenpairs (i.e., eigenvalue and corresponding eigenfunction) of the kernel function Ξ, and $\xi_{(i)}$ are independent random variables with zero mean and unit variance. In practice, the summation is truncated up to N terms for computational purpose, where N is taken such that

$$\sum_{i=1}^{N} \lambda_i \geq 0.9 \sum_{i=1}^{\infty} \lambda_i. \tag{5.1}$$

Notice that instead of 0.9, other numbers like 0.85 and 0.95 are also widely used. The notation of $F(\boldsymbol{x}, \omega)$ is then replaced with $F(\boldsymbol{x}, \boldsymbol{\xi})$, where $\boldsymbol{\xi} = (\xi_{(1)}, \xi_{(2)}, \ldots, \xi_{(N)})$. Here, we use the KL expansion to represent the

random field $a(\boldsymbol{x}, \boldsymbol{\xi})$, and we consider the nonlocal diffusion coefficient as the harmonic mean of the local diffusion coefficient: $A(\boldsymbol{x}, \boldsymbol{y}, \boldsymbol{\xi}) = 2/(a^{-1}(\boldsymbol{x}, \boldsymbol{\xi}) + a^{-1}(\boldsymbol{y}, \boldsymbol{\xi}))$ in our nonlocal model.
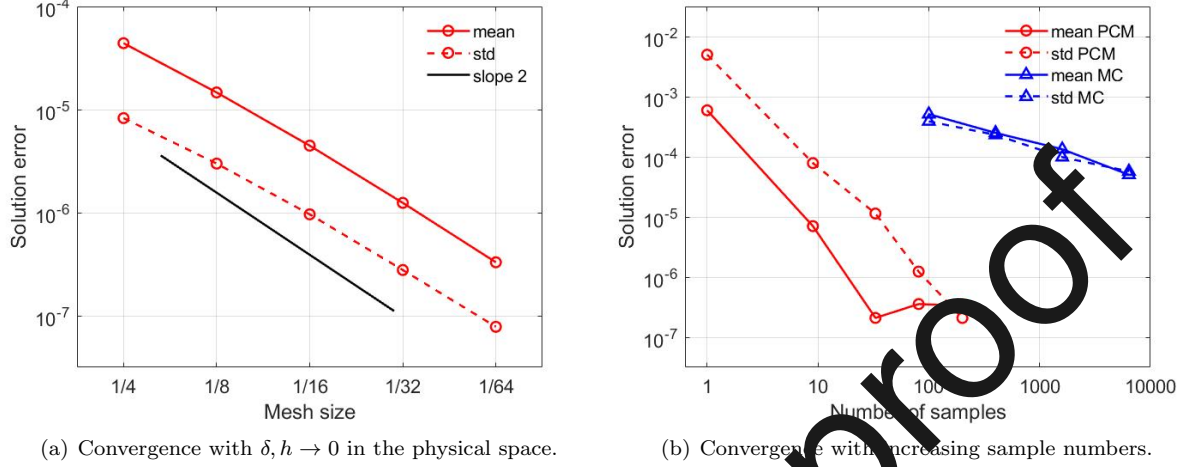
5.2. Numerical Simulations

(a) Convergence with $\delta, h \to 0$ in the physical space.

(b) Convergence with increasing sample numbers.

Figure 6: Asymptotic compatibility study of the numerical solution to the analytical local limit on randomly heterogeneous nonlocal problem with a given spatial correlation structure. Results in (a) are generated with 441 samples, which corresponds to Smolyak formulation level 5. The data points in (b) correspond to Smolyak formulation levels $\eta = 1, \cdots, 5$.

In this section, we consider the proposed approach on a randomly heterogeneous nonlocal problem with a given spatial correlation structure. We consider a 2D domain $\Omega = [-1, 1] \times [-1, 1]$ with $u^0 = 0$ on $\partial\Omega$. The local diffusivity coefficient $a(\boldsymbol{x}, \omega)$ is modeled as a random field with constant mean $a_0 = 4$ and a continuous covariance function:

$$\Xi(\boldsymbol{x}, \boldsymbol{y})(= \mathrm{Cov}(a(\boldsymbol{x}, \boldsymbol{\xi}), a(\boldsymbol{y}, \boldsymbol{\xi}))) = \sigma^2 \exp\left(-\frac{|x_{(1)} - y_{(1)}|^2}{\eta_1} - \frac{|x_{(2)} - y_{(2)}|^2}{\eta_2}\right),$$

with $\sigma = 1, \eta_1 = \eta_2 = 1$. We note σ^2 is the variance and $\eta_i, i = 1, 2$ are correlation lengths. We note that the above covariance kernel is separable, and therefore the eigenvalues and corresponding eigenfunctions in Ω can be derived by the multiplicaitons of the eigenvalues and eigenfunctions in the one-dimensional case. In particular, we first consider the eigenvalues and corresponding eigenfunctions in K–L expansion for the 1D covariance function $\Xi^{(k)}(x, y) = \sigma \exp\left(-\frac{|x-y|^2}{\eta_k}\right), k = 1, 2$ and obtain the 1D eigenpairs $(\lambda_i^{(k)}, \phi_i^{(k)})$. The random local diffusivity coefficient is then expressed as the following expansion:

$$a(\boldsymbol{x}, \boldsymbol{\xi}) = 4 + \sum_{i=1}^{N^{(1)}} \sum_{j=1}^{N^{(2)}} \sqrt{\lambda_i^{(1)}} \sqrt{\lambda_j^{(2)}} \phi_i^{(1)}(x_{(1)}) \phi_j^{(2)}(x_{(2)}) \xi_{(i,j)}.$$

In this computational example, $N^{(1)} = N^{(2)} = 2$ is required to achieve the truncation error criteria (5.1). We assume $\xi_{(i,j)}, i, j = 1, 2$, to be Gaussian random variables: $\xi_{(i,j)} \sim N(0, 1)$, then investigate the convergence of $u_{h,K}^{\delta}$ to the local limit. Note that in this problem there exists no analytical expression for the local

37

solution, we therefore generate $u^0(\boldsymbol{x}, \boldsymbol{\xi})$ numerically based on a spectral method solver. Similar as in Test 3 of Section 4.2, to provide a nonlocal Dirichlet-type boundary condition, we set $u^D(\boldsymbol{x}, \boldsymbol{\xi}) := u^0(\boldsymbol{x}, \boldsymbol{\xi})$ and apply this boundary condition on the interior boundary layer $\Omega_{-\delta}$. Since the MC method suffers from a very slow convergence and requires more than 10^7 samples to achieve a desired precision, the mean and standard deviation of the local limit is calculated with the sparse grid PCM method with 2881 samples (sparse grid level $\eta = 10$).

Numerical results are provided in Figure 6. In Figure 6(a) we demonstrate the convergence in the physical space with uniform grids $h \in \{1/4, 1/8, 1/16, 1/32, 1/64\}$ and fixed $\delta/h = 2.8$, using 441 sample points (sparse grid level $\eta = 5$). Second order convergence is observed, which verifies the analysis in Theorem 3.13. To demonstrate the convergence in the parametric space with increasing sample numbers, in Figure 6(b) we employ a fixed grid size $h = 1/64$, $\delta = 2.8h$, and show the numerical error to the local limit with sparse grid levels $\eta = 1, \cdots, 5$ in PCM. The results again indicate that comparing with MC, the sparse grid PCM achieves a better accuracy with far smaller number of samples. Although the regularity requirement of $\boldsymbol{u}^0$ in Theorem 3.13 is again not guaranteed, an algebraic convergence is still observed empirically, demonstrating the applicability of the proposed framework in engineering-oriented applications.

6. Summary and Discussion

Due to the limitation of computational resources and experimental resolutions, in many applications the physical parameters describing continuous properties of heterogeneous materials cannot be accurately characterized in all details. This problem becomes more acute in the nonlocal setting, due to its relatively lack of sparsity and correspondingly larger computational cost.

In this work we aim to consider the spatial variability of material properties in nonlocal models by solving randomly heterogeneous nonlocal diffusion problems. In particular, we have proposed an asymptotically compatible stochastic numerical method for randomly heterogeneous nonlocal diffusion problems, and provided rigorous mathematical analysis and error estimates. For spatial discretization, a meshfree discretization method with optimization-based quadrature rule is employed, which presents an up to $O(h)$ consistency error to the nonlocal solution and an $O(\delta^2)$ convergence to the local limit. On the random parametric space, a probabilistic collocation method (PCM) with sparse grids is employed to sample the stochastic process. Since the fast convergence of the sparse grid PCM approach relies on smoothness of the solution in the random parametric space, we have proved that the nonlocal solution is analytic in the input random variable and therefore guarantees an at least algebraic convergence with increasing sample numbers. This work has for the first time provided a rigorous and comprehensive mathematical framework to add uncertainty quantification analysis onto pre-existing deterministic codes for nonlocal problems with guaranteed convergence in both physical and parametric spaces.

Future directions of this research will include the development and analysis of a generalization of this approach to the nonlocal mechanics problems, such as the peridynamics. While peridynamics has been

shown to be a useful model for phase transformations and fracture problems [91, 92], most of the current work has been restricted to deterministic models. However, in these problems the material's microstructure, properties, interfacial conditions, and operating environments all cause variability in the material's response; hence it is often non-practical, if not impossible, to provide quantitative characterization for each material sample. This fact calls for a stochastic peridynamics modeling of the variability and characterization of the material responses through uncertainty quantification [40]. On the other hand, since phase transformations and fracture are both nonlinear phenomena, a development of stochastic method for nonlocal and nonlinear problems is also desired. Further studies on the meshfree methods for nonlocal models include convergence analysis for solutions with lower regularity and higher order meshfree discretizations.

Acknowledgements

References

[1] S. A. Silling, Reformulation of elasticity theory for discontinuities and long-range forces, Journal of the Mechanics and Physics of Solids 48 (1) (2000) 175–209.

[2] Z. P. Bažant, M. Jirásek, Nonlocal integral formulations of plasticity and damage: survey of progress, Journal of Engineering Mechanics 128 (11) (2002) 1119–1149.

[3] M. Zimmerman, A continuum theory with long-range forces for solids, Ph.D. thesis, Massachusetts Institute of Technology (2005).

[4] E. Emmrich, O. Weckner, Analysis and numerical approximation of an integro-differential equation modeling non-local effects in linear elasticity, Mathematics and Mechanics of Solids 12 (4) (2007) 363–384.

[5] E. Emmrich, O. Weckner, et al., On the well-posedness of the linear peridynamic model and its convergence towards the navier equation of linear elasticity, Communications in Mathematical Sciences 5 (4) (2007) 851–864.

[6] K. Zhou, Q. Du, Mathematical and numerical analysis of linear peridynamic models with nonlocal boundary conditions, SIAM Journal on Numerical Analysis 48 (5) (2010) 1759–1780.

[7] Q. Du, K. Zhou, Mathematical analysis for the peridynamic nonlocal continuum theory, ESAIM: Mathematical Modelling and Numerical Analysis 45 (02) (2011) 217–234.

[8] Q. Du, R. Lipton, T. Mengesha, Multiscale analysis of linear evolution equations with applications to nonlocal models for heterogeneous media, ESAIM: Mathematical Modelling and Numerical Analysis 50 (5) (2016) 1425–1455.

[9] I. Podlubny, Fractional differential equations: an introduction to fractional derivatives, fractional differential equations, to methods of their solution and some of their applications, Vol. 198, Academic Press, 1998.

[10] F. Mainardi, Fractional calculus and waves in linear viscoelasticity: an introduction to mathematical models, World Scientific, 2010.

[11] R. L. Magin, Fractional calculus in bioengineering, Begell House Publishers Inc., Redding, CT, 2006.

[12] N. Burch, R. Lehoucq, Classical, nonlocal, and fractional diffusion equations on bounded domains, International Journal for Multiscale Computational Engineering 9 (6).

[13] Q. Du, Z. Huang, R. B. Lehoucq, Nonlocal convection-diffusion volume-constrained problems and jump processes., Discrete & Continuous Dynamical Systems-Series B 19 (4).

[14] O. Defterli, M. D'Elia, Q. Du, M. Gunzburger, R. Lehoucq, M. M. Meerschaert, Fractional diffusion on bounded domains, Fractional Calculus and Applied Analysis 18 (2) (2015) 342–360.

[15] A. Lischke, G. Pang, M. Gulian, F. Song, C. Glusa, X. Zheng, Z. Mao, W. Cai, M. M. Meerschaert, M. Ainsworth, et al., What is the fractional laplacian?, arXiv preprint arXiv:1801.09767.

[16] Q. Du, R. Lipton, Peridynamics, fracture, and nonlocal continuum models, SIAM News 47 (3).

[17] X. Antoine, H. Barucq, Approximation by generalized impedance boundary conditions of a transmission problem in acoustic scattering, ESAIM: Mathematical Modelling and Numerical Analysis 39 (5) (2005) 1041–1059.

[18] K. Dayal, K. Bhattacharya, A real-space non-local phase-field model of ferroelectric domain patterns in complex geometries, Acta Materialia 55 (6) (2007) 1907–1917.

[19] E. W. Sachs, M. Schu, A priori error estimates for reduced order models in finance, ESAIM: Mathematical Modelling and Numerical Analysis 47 (2) (2013) 449–469.

[20] F. A. Chiarello, P. Goatin, Global entropy weak solutions for general non-local traffic flow models with anisotropic kernel, ESAIM: Mathematical Modelling and Numerical Analysis 52 (1) (2018) 163–180.

[21] H. A. Erbay, S. Erbay, A. Erkip, Convergence of a semi-discrete numerical method for a class of nonlocal nonlinear wave equations, ESAIM: Mathematical Modelling and Numerical Analysis 52 (3) (2018) 803–826.

[22] C. Bucur, E. Valdinoci, Nonlocal diffusion and applications, Vol. 20, Springer, 2016.

[23] H. You, Y. Yu, N. Trask, M. Gulian, M. D'Elia, Data-driven learning of nonlocal physics from high-fidelity synthetic data, Computer Methods in Applied Mechanics and Engineering 374 (2021) 113553.

[24] Q. Du, M. Gunzburger, R. B. Lehoucq, K. Zhou, A nonlocal vector calculus, nonlocal volume-constrained problems, and nonlocal balance laws, Mathematical Models and Methods in Applied Sciences 23 (03) (2013) 493–540.

[25] Y. Yu, F. F. Bargos, H. You, M. L. Parks, M. L. Bittencourt, G. E. Karniadakis, A partitioned coupling framework for peridynamics and classical theory: Analysis and simulation, Computer Methods in Applied Mechanics and Engineering 340 (2018) 905–931.

[26] X. Tian, Q. Du, Asymptotically compatible schemes and applications to robust discretization of nonlocal models, SIAM Journal on Numerical Analysis 52 (4) (2014) 1641–1665.

[27] M. D'Elia, Q. Du, C. Glusa, M. Gunzburger, X. Tian, Z. Zhou, Numerical methods for nonlocal and fractional models, Acta Numerica 29 (2020) 1–124.

[28] Y. Leng, X. Tian, N. Trask, J. T. Foster, Asymptotically compatible reproducing kernel collocation and meshfree integration for nonlocal diffusion, SIAM Journal on Numerical Analysis 59 (1) (2021) 88–118.

[29] M. Pasetto, Y. Leng, J.-S. Chen, J. T. Foster, P. Seleson, A reproducing kernel enhanced approach for peridynamic solutions, Computer Methods in Applied Mechanics and Engineering 340 (2018) 1044–1078.

[30] M. Hillman, M. Pasetto, G. Zhou, Generalized reproducing kernel peridynamics: unification of local and non-local meshfree methods, non-local derivative operations, and an arbitrary-order state-based peridynamic formulation, Computational Particle Mechanics 7 (2) (2020) 435–469.

[31] P. Seleson, D. J. Littlewood, Convergence studies in meshfree peridynamic simulations, Computers & Mathematics with Applications 71 (11) (2016) 2432–2448.

[32] Q. Du, Local limits and asymptotically compatible discretizations, Handbook of peridynamic modeling (2016) 87–108.

[33] N. Trask, H. You, Y. Yu, M. L. Parks, An asymptotically compatible meshfree quadrature rule for nonlocal problems with applications to peridynamics, Computer Methods in Applied Mechanics and Engineering 343 (2019) 151–165.

[34] H. You, X. Lu, N. Task, Y. Yu, An asymptotically compatible approach for neumann-type boundary condition on nonlocal problems, ESAIM: Mathematical Modelling and Numerical Analysis 54 (4) (2020) 1373–1413.

[35] H. You, Y. Yu, D. Kamensky, An asymptotically compatible formulation for local-to-nonlocal coupling problems without overlapping regions, Computer Methods in Applied Mechanics and Engineering 366 (2020) 113038.

[36] Y. Tao, X. Tian, Q. Du, Nonlocal diffusion and peridynamic models with neumann type constraints and their numerical approximations, Applied Mathematics and Computation 305 (2017) 282–298.

[37] Y. Yu, H. You, N. Trask, An asymptotically compatible treatment of traction loading in linearly elastic peridynamic fracture, Computer Methods in Applied Mechanics and Engineering 377 (2021) 113691.

[38] S. A. Silling, E. Askari, A meshfree method based on the peridynamic model of solid mechanics, Computers & structures 83 (17-18) (2005) 1526–1535.

[39] M. Bessa, J. Foster, T. Belytschko, W. K. Liu, A meshfree unification: reproducing kernel peridynamics, Computational Mechanics 53 (6) (2014) 1251–1264.

[40] J. Zhao, Z. Chen, J. Mehrmashhadi, F. Bobaru, A stochastic multiscale peridynamic model for corrosion-induced fracture in reinforced concrete, Engineering Fracture Mechanics (2020) 106969.

[41] M. Stein, Large sample properties of simulations using latin hypercube sampling, Technometrics 29 (2) (1987) 143–151.

[42] W.-L. Loh, et al., On latin hypercube sampling, Annals of statistics 24 (5) (1996) 2058–2080.

[43] B. L. Fox, Strategies for Quasi-Monte Carlo, Vol. 22, Springer Science & Business Media, 1999.

[44] H. Niederreiter, Random number generation and quasi-Monte Carlo methods, SIAM, 1992.

[45] K. A. Cliffe, M. B. Giles, R. Scheichl, A. L. Teckentrup, Multilevel monte carlo methods and applications to elliptic pdes with random coefficients, Computing and Visualization in Science 14 (1) (2011) 3–15.

[46] G. Dagan, Comment on "renormalization group analysis of macrodispersion in a directed random flow" by u. jaekel and h. vereecken, Water resources research 34 (11) (1998) 3197–3198.

[47] I. Babuska, R. Tempone, G. E. Zouraris, Galerkin finite element approximations of stochastic elliptic partial differential equations, SIAM Journal on Numerical Analysis 42 (2) (2004) 800–825.

[48] I. Babuška, R. Tempone, G. E. Zouraris, Solving elliptic boundary value problems with uncertain coefficients by the finite element method: the stochastic formulation, Computer methods in applied mechanics and engineering 194 (12-16) (2005) 1251–1294.

[49] R. G. Ghanem, P. D. Spanos, Stochastic finite elements: a spectral approach, Courier Corporation, 2003.

[50] O. Le Maıtre, O. Knio, H. Najm, R. Ghanem, Uncertainty propagation using wiener–haar expansions, Journal of computational Physics 197 (1) (2004) 28–57.

[51] H. G. Matthies, A. Keese, Galerkin methods for linear and nonlinear elliptic stochastic partial differential equations, Computer methods in applied mechanics and engineering 194 (12-16) (2005) 1295–1331.

[52] D. Xiu, G. E. Karniadakis, The wiener–askey polynomial chaos for stochastic differential equations, SIAM journal on scientific computing 24 (2) (2002) 619–644.

[53] X. Wan, G. E. Karniadakis, An adaptive multi-element generalized polynomial chaos method for stochastic differential equations, Journal of Computational Physics 209 (2) (2005) 617–642.

[54] D. Xiu, J. S. Hesthaven, High-order collocation methods for differential equations with random inputs, SIAM Journal on Scientific Computing 27 (3) (2005) 1118–1139.

[55] F. Nobile, R. Tempone, C. G. Webster, An anisotropic sparse grid stochastic collocation method for partial differential equations with random input data, SIAM Journal on Numerical Analysis 46 (5) (2008) 2411–2442.

[56] X. Ma, N. Zabaras, An adaptive hierarchical sparse grid collocation algorithm for the solution of stochastic differential equations, Journal of Computational Physics 228 (8) (2009) 3084–3113.

[57] G. Zhang, M. Gunzburger, Error analysis of a stochastic collocation method for parabolic partial differential equations with random input data, SIAM Journal on Numerical Analysis 50 (4) (2012) 1922–1940.

[58] G. Lin, A. M. Tartakovsky, An efficient, high-order probabilistic collocation method on sparse grids for three-dimensional flow and solute transport in randomly heterogeneous porous media, Advances in Water Resources 32 (5) (2009) 712–722.

[59] G. Rozza, D. B. P. Huynh, A. T. Patera, Reduced basis approximation and a posteriori error estimation for affinely parametrized elliptic coercive partial differential equations, Archives of Computational Methods in Engineering 15 (3) (2007) 1.

[60] G. Rozza, K. Veroy, On the stability of the reduced basis method for stokes equations in parametrized domains, Computer methods in applied mechanics and engineering 196 (7) (2007) 1244–1260.

[61] P. Chen, A. Quarteroni, G. Rozza, Comparison between reduced basis and stochastic collocation methods for elliptic problems, Journal of Scientific Computing 59 (1) (2014) 187–216.

[62] P. Chen, A. Quarteroni, G. Rozza, A weighted reduced basis method for elliptic partial differential equations with random input data, SIAM Journal on Numerical Analysis 51 (6) (2013) 3163–3185.

43

[63] H. C. Elman, Q. Liao, Reduced basis collocation methods for partial differential equations with random coefficients, SIAM/ASA Journal on Uncertainty Quantification 1 (1) (2013) 192–217.

[64] Q. Guan, M. Gunzburger, C. G. Webster, G. Zhang, Reduced basis methods for nonlocal diffusion problems with random input data, Computer Methods in Applied Mechanics and Engineering 317 (2017) 746–770.

[65] Q. Du, X. Tian, C. Wright, Y. Yu, Nonlocal trace spaces and extension results for nonlocal calculus, Preprint.

[66] T. Mengesha, Q. Du, The bond-based peridynamic system with dirichlet-type volume constraint, Proc. Roy. Soc. Edinburgh Sect. A 144 (1) (2014) 161–186.

[67] M. Gunzburger, R. B. Lehoucq, A nonlocal vector calculus with application to nonlocal boundary value problems, Multiscale Modeling & Simulation 8 (5) (2010) 1581–1598.

[68] R. Lipton, Dynamic brittle fracture as a small horizon limit of peridynamics, Journal of Elasticity 117 (1) (2014) 21–50.

[69] J. Zhao, S. Jafarzadeh, Z. Chen, F. Bobaru, An algorithm for imposing local boundary conditions in peridynamic models on arbitrary domains.

[70] H. Lee, Q. Du, Second order accurate dirichlet boundary conditions for linear nonlocal diffusion problems, arXiv preprint arXiv:2108.11817.

[71] F. Scabbia, M. Zaccariotto, U. Galvanetto, A novel and effective way to impose boundary conditions and to mitigate the surface effect in state-based peridynamics, International Journal for Numerical Methods in Engineering 122 (20) (2021) 5773–5811.

[72] M. Foss, P. Radu, Y. Yu, Convergence analysis and numerical studies for linearly elastic peridynamics with dirichlet-type boundary conditions, arXiv preprint arXiv:2106.13878.

[73] M. D'Elia, X. Tian, Y. Yu, A physically consistent, flexible, and efficient strategy to convert local boundary conditions into nonlocal volume constraints, SIAM Journal on Scientific Computing 42 (4) (2020) A1935–A1949.

[74] M. D'Elia, Y. Yu, On the prescription of boundary conditions for nonlocal poisson's and peridynamics models, arXiv preprint arXiv:2107.04450.

[75] H. Tran, C. G. Webster, G. Zhang, Analysis of quasi-optimal polynomial approximations for parameterized pdes with deterministic and stochastic coefficients, Numerische Mathematik 137 (2) (2017) 451–493.

[76] A. Cohen, R. Devore, C. Schwab, Analytic regularity and polynomial approximation of parametric and stochastic elliptic pde's, Analysis and Applications 9 (01) (2011) 11–47.

[77] F. Bobaru, M. Yang, L. F. Alves, S. A. Silling, E. Askari, J. Xu, Convergence, adaptive refinement, and scaling in 1d peridynamics, International Journal for Numerical Methods in Engineering 77 (6) (2009) 852–877.

[78] S. Silling, R. Lehoucq, Peridynamic theory of solid mechanics, Advances in Applied Mechanics 44 (1) (2010) 73–166.

[79] H. Wendland, Local polynomial reproduction and moving least squares approximation, IMA Journal of Numerical Analysis 21 (1) (2001) 285–300.

[80] H. Wendland, Scattered data approximation, Vol. 17, Cambridge university press, 2004.

[81] L. C. Evans, Partial Differential Equations (Graduate Studies in Mathematics, Vol. 19), American Mathematical Society, Providence, Rhode Island, 2002.

[82] A. Brudnyi, et al., Methods of geometric analysis in extension and trace problems: volume 1, Vol. 102, Springer Science & Business Media, 2011.

[83] M. Tatang, G. McRae, Direct treatment of uncertainty in models of reaction and transport, Technical report, MIT Tech. Rep.

[84] A. Keese, H. Matthies, et al., Numerical methods and smolyak quadrature for nonlinear stochastic partial differential equations.

[85] S. A. Smolyak, Quadrature and interpolation formulas for tensor products of certain classes of functions, in: Doklady Akademii Nauk, Vol. 148, Russian Academy of Sciences, 1963, pp. 1042–1045.

[86] E. Novak, K. Ritter, High dimensional integration of smooth functions over cubes, Numerische Mathematik 75 (1) (1996) 79–97.

[87] E. Novak, K. Ritter, Simple cubature formulas with high polynomial exactness, Constructive approximation 15 (4) (1999) 499–522.

[88] V. Dzjadyk, V. Ivanov, On asymptotics and estimates for the uniform norms of the lagrange interpolation polynomials corresponding to the Chebyshev nodal points, Analysis Mathematica 9 (2) (1983) 85–97.

[89] S. A. Silling, Propagation of a stress pulse in a heterogeneous elastic bar, Journal of Peridynamics and Nonlocal Modeling (2021) 1–21.

[90] H. You, Y. Yu, S. Silling, M. D'Elia, Data-driven learning of nonlocal models: from high-fidelity simulations to constitutive laws, AAAI Spring Symposium: MLPS.

45

[91] K. Dayal, K. Bhattacharya, Kinetics of phase transformations in the peridynamic formulation of continuum mechanics, Journal of the Mechanics and Physics of Solids 54 (9) (2006) 1811–1842.

[92] P. Diehl, S. Prudhomme, M. Lévesque, A review of benchmark experiments for the validation of peridynamics models, Journal of Peridynamics and Nonlocal Modeling 1 (1) (2019) 14–35.

Declaration of interests

X The authors declare that they have no known competing financial interests or personal relationships that could have appeared to influence the work reported in this paper.

☐The authors declare the following financial interests/personal relationships which may be considered as potential competing interests:

Yiming Fan: Software, Methodology, Programming.
Xiaochuan Tian: Analysis, Writing
Xiu Yang: Software, Editing.
Xingjie Li: Software, Editing.
Clayton Webster: Supervision.
Yue Yu: Supervision, Conceptualization, Writing.